Applied Mathematical Modelling 39 (2015) 2740–2762

Contents lists available at ScienceDirect

Applied Mathematical Modelling

journal homepage: www.elsevier.com/locate/apm

Transient quasi-static Ritz vector (TQSRV) method by Krylov subspaces and eigenvectors for efficient contact dynamic finite element simulation

Gil Ho Yoon [a,*], Jun Hwan Kim [b], Kwang Ok Jung [b], Jae Won Jung [b]

[a] School of Mechanical Engineering, Hanyang University, Republic of Korea
[b] Graduate School of Mechanical Engineering, Hanyang University, Republic of Korea

ARTICLE INFO

Article history:
Received 19 November 2013
Received in revised form 3 July 2014
Accepted 16 October 2014
Available online 23 November 2014

Keywords:
Model order reduction method
Transient quasi-static Ritz vector method
Ritz vector method
Quasi-static Ritz vector method

ABSTRACT

This paper presents a novel model order reduction (MOR) method called the transient quasi-static Ritz vector (TQSRV) method for efficient transient finite element (FE) analysis. Comparing with frequency response analysis, linear transient FE analysis with a fixed time step takes less computation time as an effective dynamic stiffness matrix assembled before time marching procedure is factorized once. Nevertheless as the number of degrees of freedom of a FE model has been dramatically increased for accurate engineering simulation, even the state-of-the-art computer and software often face their limitations. For fast but accurate transient FE analysis, we present a new MOR scheme called the TQSRV method with Krylov bases spanned at multiple angular velocities and several lowest eigenvectors. By calculating transient responses of reduced FE models and comparing it with the responses of full FE models, the effectiveness and accuracy of the TQSRV method are demonstrated.

1. Introduction

In this research, a new mathematical model order reduction scheme named as the transient quasi-static Ritz vector method (TQSRV method) is developed for efficient transient finite element analysis [1,2]. Despite the recent radical developments of high performance computer hardware and computer aided engineering software, it is still difficult and challenging to efficiently calculate the responses of complex manifold structures such as automotive, ship, and complex acoustic system as shown in Fig. 1 with fine incremental time (transient FE analysis) or fine incremental frequency interval (frequency response analysis or FRA). For FRA, the issue in the computational time can be overcome efficiently and effectively by applying the elaborated model order reduction (MOR) schemes such as Guyan reduction, the mode superposition method (MS method), the Ritz vector method (RV method), the quasi-static Ritz vector method (QSRV method) and the multifrequency quasi-static Ritz vector method (MQSRV) method [3]. Compared with the number of the researches of the MOR method for FRA, it is likely that there are few researches applying the MOR methods to transient FE analysis for the computational efficiency [4–7]. In [4], the concept of the reduction bases was proposed with Ritz vectors in transient FE analysis. In [5], the load-dependent method and the mode-displacement method are proposed based on the superposition of eigenvectors. For the efficient seismic analysis of elasto-plastic, a computational algorithm based on the pseudo-force method and the

* Corresponding author.
E-mail addresses: ghy@hanyang.ac.kr, gilho.yoon@gmail.com (G.H. Yoon).

http://dx.doi.org/10.1016/j.apm.2014.10.059
0307-904X/

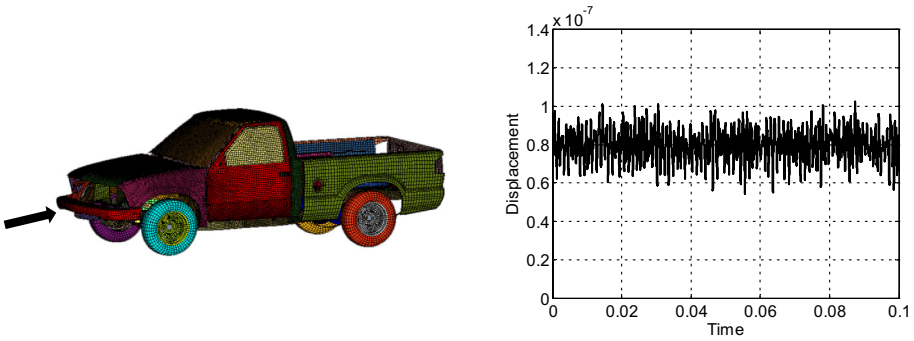

Fig. 1. Transient FE analysis for complex manifold structure.

tangent spectrum method was proposed in [6]. In [7], the reduced order model with open-source software, MOR4ANSYS, was used to calculate the transient response of MEMS devices. In [8], the quasi-static Ritz vector (QSRV) method was proposed and by extending their ideas, a new MOR idea was developed and applied for frequency dependent acoustic analysis in [3,9]. In addition the developed MOR techniques also have been used for structural optimization (See [10–12] for more details) and for the damage detection and health monitoring of large-scale structure (See [13] and references therein). Furthermore in electrical engineering, there are many relevant researches applying the concept of the MOR method for efficient analysis [14–23]. This research focuses on the new development of a novel MOR method named as the transient quasi-static Ritz vector (TQSRV) method whose bases are Krylov subspace bases and eigenvectors for efficient transient FE analysis. Thus this research focuses the following subjects.

Research object 1: The development of the new reduction bases of the TQSRV method with Krylov subspaces and eigenvectors.

Research object 2: The efficient transient FE analysis with the present TQSRV method including the contact condition.

The currently available MOR methods such as MS, RV, QSRV and MQSRV methods need more contributions from mathematicians and engineers for the application toward transient FE analysis [1]. Unlike FRA procedure requiring quite a lot inversions of effective stiffness matrices, commonly implicit or explicit transient FE analysis for linear structure with a fixed time step only requires one time effective stiffness matrix factorization [4,6,24]. Therefore compared with the existing solution procedures of FRA without any MOR method, it is generally possible to conduct transient FE analysis efficiently. However, with a manifold FE model having a lot of degrees of freedom, it also takes a lot of time to compute transient response with implicit or explicit time marching procedure. Recently with the help of the advanced computer hardware, a multithread parallelization process can be employed to reduce the computational burden involved with transient analysis or FRA with vector addition, vector–vector multiplication, vector–matrix multiplication, and forward substitution and backward substitution. On the other hands, in order to shorten the computational time involved at the time-marching procedure of transient FE analysis, this research finds out that the concept of the MOR method developed mainly for FRA can be employed. As the existing MOR schemes are not effective in transient FE analysis from accuracy and computation point of view, we develop a new MOR method named as the TQSRV method as shown in Fig. 2. The conventional MOR schemes being developed for FRA not for transient FE analysis, they are not necessary accurate enough to be applied from engineering point of view. Furthermore we consider its application for the contact finite element analysis.

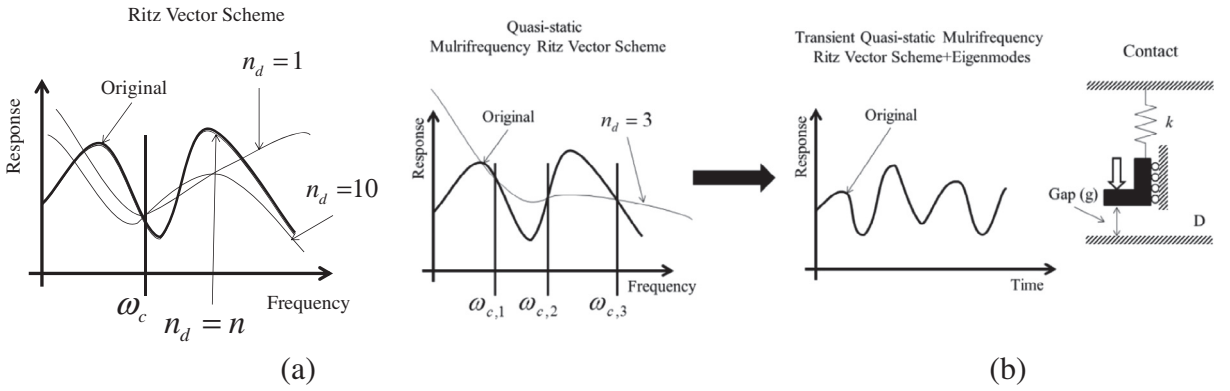

Fig. 2. The Ritz vector method and the multifrequency Ritz vector method for frequency response analysis and its application to the transient contact finite element analysis.

Table 1
the standard procedure of Newmark scheme.

Set initial position, velocity and acceleration
Calculate and factorize the effective stiffness matrix ($\mathbf{K}_{\text{Eff}}$(LU decomposition))
for time step
$t_{n+1} = t_n + \Delta t$
Calculate the current effective force $\left(\mathbf{F}_{n+1}^{\text{Eff}}\right)$
calculate the current displacements $\left(\mathbf{K}_{\text{Eff}}\mathbf{X}_{n+1}^{=}\mathbf{F}_{n+1}^{\text{Eff}}\right)$
update the accelerations
update the velocities
end

The present TQSRV scheme shares the basic concepts with the established MOR schemes that structural responses in time domain can be spanned or approximated with "good" bases with a few unknown variables. As the other MOR schemes concerns, it is an important subject to systematically calculate the "good" bases playing a critical role in expanding original structural response accurately. In the present TQSRV method, the bases of the MQSRV method and the MS method are integrated together; the Ritz bases of the MQSRV method are the pseudo static displacements calculated at multi-frequencies and the bases of the MS method are some lowest eigenvectors of a FE model. By combining the bases of the two schemes, we found that they can provide considerably much more accurate predictions for transient structural responses of complex FE models than the common MOR methods.

The layout of the paper is composed as follows. First of all, the basic concepts of the some MOR schemes such as the RV method, the QSRV method and the MQSRV method and the MS method are presented after the short descriptions of the transient FE formulation based on the Newmark scheme which is one of implicit FE schemes. After that the TQSRV method by combing the bases of the MQSRV method and the MS method is presented. Using some analysis benchmark examples of two and three dimensional structures, the efficiency and characteristics of the present TQSRV method are numerically studied and compared. And the new application of the present TQSRV method for the transient FE analysis with the contact condition is presented. Finally our findings and some topics for future research are summarized and discussed in the conclusion.

2. Transient FE analysis and MOR scheme

2.1. Transient FE analysis

Without loss of generality, the time varying response of a linear solid structure with time varying force **F**is calculated by the second Newton's equation as follows:

$$\mathbf{M}\ddot{\mathbf{X}} + \mathbf{C}\dot{\mathbf{X}} + \mathbf{K}\mathbf{X} = \mathbf{F}, \tag{1}$$

where **M**, **C** and **K** represent the mass matrix, the damping matrix and the stiffness matrix with appropriate boundary conditions, respectively [5,22]. The time-varying displacements, velocities, and accelerations of a structure are denoted by $\mathbf{X}, \dot{\mathbf{X}}$, and $\ddot{\mathbf{X}}$, respectively. Because the studying of geometrically or materially nonlinear structure is too involved a subject to be considered for the MOR scheme, **M**, **C** and **K** are assumed to be independent on structural displacements and not to be changed with respect to time; the application for contact nonlinearity is developed later. For the sake of simplicity, the Rayleigh damping is assumed with the damping coefficients α_r and β_r in Eq. (2).

$$\mathbf{C} = \alpha_r\mathbf{M} + \beta_r\mathbf{M}. \tag{2}$$

To solve this second order differential Eq. (1), the Newmark scheme which is a single-step implicit time integration scheme or a classical time-stepping algorithm popular in structural analysis is implemented [5,22]. In this Newmark scheme, the current displacements and the velocities are approximated as follows:

$$t_{n+1} = t_n + \Delta t, \tag{3}$$

$$\mathbf{X}_{n+1} = \mathbf{X}_n + \Delta t\dot{\mathbf{X}}_n + \Delta t^2\left(\left(\frac{1}{2} - \beta\right)\ddot{\mathbf{X}}_n + \beta\ddot{\mathbf{X}}_{n+1}\right), \tag{4}$$

$$\dot{\mathbf{X}}_{n+1} = \dot{\mathbf{X}}_n + \Delta t\left((1-\gamma)\ddot{\mathbf{X}}_n + \gamma\ddot{\mathbf{X}}_{n+1}\right), \tag{5}$$

where the structural displacements, the velocities and the acceleration at time t_n are denoted by $\mathbf{X}_n, \dot{\mathbf{X}}_n$, and $\ddot{\mathbf{X}}_n$, respectively. The time indication, t_n, is used for the nth time step and the time increment is Δt (See [5,22] for more details). The parameters, β and γ, control the characteristics of Newmark scheme such as the accuracy, the numerical stability, and the amount of algorithm damping of Newmark scheme. Depending on the magnitudes of the variables, β and γ, several algorithm

variations such as the average acceleration, the linear acceleration, the Fox-Goodwin, and the Hilber–Hughes–Taylor method can be possible. Substitution of (4) and (5) into (1) for $\mathbf{X}_n$ and $\dot{\mathbf{X}}_n$ provides the standard procedure of the Newmark algorithm (Table 1).

In detail, the following equations are used for the stiffness matrix, the vectors and the corrector (update) procedures of Table 1.

$$\ddot{\mathbf{X}}_0 = \mathbf{M}^{-1}\left(\mathbf{F}_0 - \mathbf{K}\mathbf{X}_0 - [\mathbf{C}]\dot{\mathbf{X}}_0\right), \tag{6}$$

$$\mathbf{K}_{\text{Eff}}\mathbf{X}_{n+1} = \mathbf{F}^{\text{Eff}}_{n+1}, \tag{7}$$

$$\mathbf{K}_{\text{Eff}} = \mathbf{K} + \frac{1}{\beta(\Delta t)^2}\mathbf{M} + \frac{\gamma}{\beta(\Delta t)}\mathbf{C}, \tag{8}$$

$$\mathbf{F}^{\text{Eff}}_{n+1} = \mathbf{F}_{n+1} + \mathbf{M}\left\{\frac{1}{\beta(\Delta t)^2}\mathbf{X}_n + \frac{1}{\beta(\Delta t)}\dot{\mathbf{X}}_n + \left(\frac{1}{2\beta} - 1\right)\ddot{\mathbf{X}}_{n+1}\right\} + \mathbf{C}\left\{\frac{\gamma}{\beta(\Delta t)}\mathbf{X}_n + \left(\frac{\gamma}{\beta} - 1\right)\dot{\mathbf{X}}_n + \Delta t\left(\frac{\gamma}{2\beta} - 1\right)\ddot{\mathbf{X}}_n\right\}, \tag{9}$$

$$\ddot{\mathbf{X}}_{n+1} = \frac{1}{\beta\Delta t^2}(\mathbf{X}_{n+1} - \mathbf{X}_n) - \frac{1}{\beta\Delta t}\dot{\mathbf{X}}_n - \left(\frac{1}{2\beta} - 1\right)\ddot{\mathbf{X}}_n, \tag{10}$$

$$\dot{\mathbf{X}}_{n+1} = \dot{\mathbf{X}}_n + \Delta t(1-\gamma)\ddot{\mathbf{X}}_n + \gamma\Delta t\ddot{\mathbf{X}}_{n+1} : \text{Same as the Eq. (5)}, \tag{11}$$

where the effective stiffness matrix, the effective force at the $(n+1)$th time step and the external force of the $(n+1)$th time step of Newmark scheme are denoted by $\mathbf{K}_{\text{Eff}}, \mathbf{F}^{\text{Eff}}_{n+1}$, and $\mathbf{F}_{n+1}$,respectively. The external force at the 0th time step is $\mathbf{F}_0$.

It is important to notice that unlike FRA, the Newmark procedure only requires one matrix inversion or the *LU* decomposition of the dynamic stiffness matrix. In practice due to the memory shortage, it is common to use the *LU* decomposition rather than to save the inverse matrix of the dynamic stiffness matrix. Therefore compared with FRA whose stiffness matrices are dependent on exciting angular velocity, it is regarded that the structural response of a transient FE analysis can be effectively calculated in transient FE analysis. Nevertheless if we are concerned about a FE model with a lot of DOFs, the time marching procedure from (7)–(11) also takes a lot of time and the computation times becomes problematic.

2.2. Introduction of the MOR scheme

For accurate response calculations, the number of degrees of freedom of a computational model has been significantly increased. Therefore we can easily image refined FE or FD meshes hard to be solved even by the most advanced and state-of-the-art computational system within a moderate computation time. In FRA analysis, often these limitations are overcome by the introduction of a MOR scheme reducing the size of assembled stiffness and mass matrices but not decreasing the number of degrees of freedom [6–8,14,16,19–23,25–34]. So far many MOR schemes have been developed such as Guyan reduction method [34], the MS method [1], the RV method, the QSRV method, the MQSRV method and Proper Orthogonal Decomposition method. Except the Guyan reduction scheme, the other MOR schemes are similar to each other. By approximating the original structural response with the approximated response, $\mathbf{\Psi Q}$, the MOR methods reduce the size of linear algebra system by transforming a large set of system equations into a small set of equation [3,10]. From a mathematical point of view, the approximated response, $\mathbf{X}_A$, of the original response $\mathbf{X}$ can be defined as follows:

$$\mathbf{A}\mathbf{X} = \mathbf{B}, \tag{12}$$

$$\mathbf{X} \cong \mathbf{X}_A = \mathbf{\Psi}\mathbf{Q}, \tag{13}$$

$$\mathbf{\Psi} = [\boldsymbol{\varphi}_1, \boldsymbol{\varphi}_2, \ldots, \boldsymbol{\varphi}_{n_d}](n_d \leqslant n_s), \tag{14}$$

where $\mathbf{A}$ and $\mathbf{B}$ denote an arbitrary $n_s \times n_s$system matrix and a $n_s \times 1$ force vector that vary depending on a mechanical system of interest; the number of degrees of freedom of a system is n_s and the number of retained degrees of freedom is n_d. In (13), $\mathbf{\Psi}$ is the frequency dependent basis vector of order n_d and $\mathbf{Q}$ are the retained unknown variables for the basis $\boldsymbol{\varphi}_i$. By premultiplying $\mathbf{\Psi}^{\text{T}}$ into the original dynamic Eq. (12), the following reduced equation with the order n_d is obtained:

$$\underbrace{\{\mathbf{\Psi}^{\text{T}}\mathbf{A}\mathbf{\Psi}\}}_{n_d\times n_d}\underbrace{\mathbf{Q}}_{n_d\times 1} = \underbrace{\mathbf{\Psi}^{\text{T}}\mathbf{B}}_{n_d\times 1}. \tag{15}$$

By solving the above reduced system with the order n_d for $\mathbf{Q}$, the approximate solution $\mathbf{X}_A$ is recovered using Eq. (13). In most MOR methods, to reduce the computation time, it is common to use a small number of bases ($n_d \ll n_s$).

2.2.1. The mode superposition method (MS method)

From an engineering and scientific point of view, one of the most popular reduction bases, $\mathbf{\Psi}$, of Eq. (14) may be the eigenvectors of an original dynamic system. In the MS method, several lowest eigenvectors are selected depending on frequency domains of interest, called cutoff frequency (See [1,10] or any finite element book about dynamic analysis). One of the benefits of this MS method is that the eigenvalues of a reduced system are exactly same as those of the original dynamic system. Therefore, engineer or scientist can predict the accuracy of the reduced dynamic system by considering the number of eigenvectors and can easily increase the accuracy of the MS method in FRA by considering additional eigenvectors.

In the MS method, for the jth natural angular velocity ω_j and the associate jth eigenvectors $\boldsymbol{\varphi}_j$ $(j = 1, \ldots, n_d)$, the following eigenvalue problem with a mass stiffness matrix, $\mathbf{M}$, and a stiffness matrix, $\mathbf{K}$, is solved.

$$\boldsymbol{\varphi}_j^{\mathrm{T}}\left[\mathbf{K} - \omega_j^2\mathbf{M}\right]\boldsymbol{\varphi}_j = 0 \quad (j = 1, \ldots, n_d, \quad n_d \leqslant n_s, \quad Rank(\mathbf{K}) = n_s), \tag{16}$$

$$\omega_1 \leqslant \omega_2 \ldots \omega_{n_d-1} \leqslant \omega_{n_d}, \tag{17}$$

With the retained n_d bases, the transformation matrix $\mathbf{\Psi}$ can be defined as follows:

$$\mathrm{MSmethod}: \mathbf{\Psi} = [\boldsymbol{\varphi}_1, \boldsymbol{\varphi}_2, \ldots, \boldsymbol{\varphi}_{n_d}], \tag{18}$$

$$\mathbf{\Psi}^{\mathrm{T}}\mathbf{M}\mathbf{\Psi} = \mathbf{I}_{n_d \times n_d}, \tag{19}$$

$$\mathbf{\Psi}^{\mathrm{T}}\mathbf{K}\mathbf{\Psi} = \begin{bmatrix} \omega_1^2 & \cdots & 0 \\ \vdots & \ddots & 0 \\ 0 & 0 & \omega_{n_d}^2 \end{bmatrix}, \tag{20}$$

$$\mathbf{\Psi}^{\mathrm{T}}\mathbf{C}\mathbf{\Psi} = \alpha_r\mathbf{I}_{n_d \times n_d} + \beta_r \begin{bmatrix} \omega_1^2 & \cdots & 0 \\ \vdots & \ddots & 0 \\ 0 & 0 & \omega_{n_d}^2 \end{bmatrix}. \tag{21}$$

By solving the simple algebraic Eq. (22), the structural response $\mathbf{X}$ for the excitation frequency ω can be obtained. Note that it is a response for FRA not for transient analysis and the transient response cannot be calculated analytically.

$$\mathbf{X}(\omega) \cong \mathbf{X}_A(\omega) = \sum_{e=1}^{n_d} q_e\boldsymbol{\varphi}_e \quad , \quad q_e = \frac{\boldsymbol{\varphi}_e^{\mathrm{T}}\mathbf{F}_\omega}{\omega_e^2 - \omega^2 + (\alpha_r + \beta_r\omega_e^2)\omega\, \boldsymbol{i}}, \tag{22}$$

where $\mathbf{F}_\omega$ is the force vector at the excitation frequency. To denote the solution and the approximate solution in frequency domain, $\mathbf{X}(\omega)$ and $\mathbf{X}_A(\omega)$ are employed.

Although the MS method is very simple and robust for most engineering problems, the convergence is relatively slow due to the requirement of many eigenmodes. When only some of eigenmodes are included and transient response is mainly represented by pseudo-static loading, this approach may fail to give an precise solution. This can be illustrated by assuming a system with the solution in the form of the combination of a single particular frequency and a constant.

$$X_p = \underbrace{A\sin(\omega_p t)}_{\substack{\text{Dynamic} \\ \text{Contribution}}} + \underbrace{B}_{\substack{\text{Static} \\ \text{Contribution}}}, \tag{23}$$

where arbitrary constants are A and B and the particular angular velocity contributing the dynamic response X_p is ω_p. Although the first dynamic contribution of the above solution can be described by only one angular velocity, ω_p, the MS method requires many eigenmodes to represent the static contribution because of the step response B. To overcome this shortage, the mode acceleration method was proposed as a computational variation of the static correction method. The basic formulation of the method is to include some additional terms as (24) in order to improve the approximated responses for low frequencies.

$$\mathbf{X} \cong \mathbf{X}_A = \mathbf{\Psi}Q + \mathbf{X}_{correct} \text{ with } \dot{\mathbf{X}}_{correct} = \ddot{\mathbf{X}}_{correct} = \mathbf{0}, \tag{24}$$

where the correction term is denoted by $\mathbf{X}_{correct}$. The correction term is given as

$$\mathbf{X}_{correct} = \left(\mathbf{K}^{-1} - \sum_{j=1}^{n_d} \frac{\boldsymbol{\varphi}_j\boldsymbol{\varphi}_j^{\mathrm{T}}}{\omega_j^2}\right)\mathbf{F}^{-1}. \tag{25}$$

2.2.2. The quasi-static Ritz vector method (QSRV method: shifted Ritz vector method)

As an alternative of the MS method, the Ritz vector (RV) method and the quasi-static Ritz vector (QSRV) method have been developed [16,22,34]. The QSRV method constructs its reduction bases $\mathbf{\Psi}$ by considering the external force $\mathbf{F}$, the mass

matrix **M**, and the stiffness matrix **K** [8,10,33]. The order m Krylov subspace κ_m generated by an arbitrary matrix **A** and an arbitrary vector **B** is the linear subspace as follows:

$$\kappa_m(\mathbf{A},\mathbf{B}) = \mathrm{span}\{\mathbf{B}, \mathbf{AB}, \mathbf{A}^2\mathbf{B}, \ldots, \mathbf{A}^{m-1}\mathbf{B}\}. \tag{26}$$

For the practical computational implementation of the QSRV method with the Krylov subspace of (26), the bases are generated through the following procedures [8,10,33,35].

$$\boldsymbol{\varphi}_1^* \equiv (\mathbf{K} - \omega_c^2\mathbf{M})^{-1}\mathbf{F} \quad (LU \text{ decomposition}), \tag{27}$$

$$\boldsymbol{\varphi}_1 = \frac{1}{\sqrt{\boldsymbol{\varphi}_1^{*\mathrm{T}}\mathbf{M}\varphi_1^*}}\boldsymbol{\varphi}_1^*, \tag{28}$$

$$\text{Krylov subspace}: \boldsymbol{\varphi}_j^* \equiv (\mathbf{K} - \omega_c^2\mathbf{M})^{-1}(\mathbf{M}\varphi_{j-1}) \quad (LU \text{ decomposition}), \tag{29}$$

$$\text{Orthogonalization}: \boldsymbol{\varphi}_j^{**} \equiv \boldsymbol{\varphi}_j^* - \sum_{k=1}^{j-1}(\boldsymbol{\varphi}_k^{\mathrm{T}}\mathbf{M}\varphi_j^*)\boldsymbol{\varphi}_k, \tag{30}$$

$$\text{Normalization}: \boldsymbol{\varphi}_j = \frac{1}{\sqrt{\boldsymbol{\varphi}_j^{**\mathrm{T}}\mathbf{M}\varphi_j^{**}}}\boldsymbol{\varphi}_j^{**}, \tag{31}$$

where ω_c is the center angular velocity of interest. If ω_c is set to zero, the QSRV method becomes the RV method exactly. Here it should be emphasized that the above procedures are formulated based on the mass orthogonalization and the mass normalization process. We found that the following RV procedures from (32) to (36) are also possible without the mass orthonormalization process.

$$\boldsymbol{\varphi}_1^* \equiv (\mathbf{K} - \omega_c^2\mathbf{M})^{-1}\mathbf{F} \quad (LU \text{ decomposition}), \tag{32}$$

$$\boldsymbol{\varphi}_1 = \frac{1}{\sqrt{\boldsymbol{\varphi}_1^{*\mathrm{T}}\boldsymbol{\varphi}_1^*}}\boldsymbol{\varphi}_1^* \quad (\text{Without the mass normalization}), \tag{33}$$

$$\boldsymbol{\varphi}_j^* \equiv (\mathbf{K} - \omega_c^2\mathbf{M})^{-1}(\mathbf{M}\boldsymbol{\varphi}_{j-1}) \quad (LU \text{ decomposition}), \tag{34}$$

$$\boldsymbol{\varphi}_j^{**} \equiv \boldsymbol{\varphi}_j^* - \sum_{k=1}^{j-1}(\boldsymbol{\varphi}_k^{\mathrm{T}}\boldsymbol{\varphi}_j^*)\boldsymbol{\varphi}_k \quad (\text{Without the mass orthogonalization}), \tag{35}$$

$$\text{Normalization}: \boldsymbol{\varphi}_j = \frac{1}{\sqrt{\boldsymbol{\varphi}_j^{**\mathrm{T}}\boldsymbol{\varphi}_j^{**}}}\boldsymbol{\varphi}_j^{**} \quad (\text{Without the mass normalization}). \tag{36}$$

After building the bases of the QSRV method, the structural response **X** is approximated again.

$$\mathbf{X} \cong \mathbf{X}_A = \boldsymbol{\Psi}\mathbf{Q}. \tag{37}$$

2.2.3. The multifrequency quasi-static Ritz vector method (MQSRV method)

Recently for the engineering application of Krylov subspace bases to frequency dependent acoustic system, the multifrequency quasi-static Ritz vector method was proposed [3,10]. It is a basic mathematical assumption of the Krylov subspace method that mass and stiffness matrices remain constants in time or in frequency. With this assumption, the moment matching theory can be applied for the power series of the response with respect to angular velocity. Often however there are some mechanical systems whose mass matrix, stiffness matrix and force vector are frequency dependent and Krylov subspace bases may not be applicable to these frequency dependent systems. For the MOR application of frequency dependent systems, the combinations of Krylov subspace bases constructed at multiple center frequencies were proposed as follows:

$$\boldsymbol{\varphi}_{s,1} \equiv \left(\mathbf{K}(\omega_{c,s}) - \omega_{c,s}^2\mathbf{M}(\omega_{c,s})\right)^{-1}\mathbf{F}(\omega_{c,s}) \tag{38}$$

$$\boldsymbol{\varphi}_{s,j} \equiv \left(\mathbf{K}(\omega_{c,s}) - \omega_{c,s}^2\mathbf{M}(\omega_{c,s})\right)^{-1}(\mathbf{M}(\omega_{c,s})\boldsymbol{\varphi}_{s,j-1}) \tag{39}$$

$$\omega_{c,s}\left(=\frac{\omega_{s,start}+\omega_{s,end}}{2}\right), \quad s = 1,\ldots,nf, \quad j = 1,\ldots,n_{d,s} \tag{40}$$

where the starting frequency, the ending frequency, and the center frequency of the sth frequency domain are denoted by $\omega_{s,start}, \omega_{s,end}$, and $\omega_{c,s}$, respectively and where the total number of considered frequency domains is nf. The number of bases calculated for the sth frequency domain is denoted by $n_{d,s}$. Although almost all the procedures are the same as those proposed in [3,15,22,24], the stiffness and mass matrices and the force vector are made to be dependent on the angular speed. The orthonormalization procedure is not applied due to the frequency-dependent mass matrix. Finally, using the above simplified procedure, the following bases are constructed for the bases of the MQSRV method.

$$\mathbf{Q} = \left[\underbrace{\boldsymbol{\varphi}_{1,1} \cdots \boldsymbol{\varphi}_{1,n_{d,1}}}_{\text{the 1st domain}}, \underbrace{\boldsymbol{\varphi}_{1,2} \cdots \boldsymbol{\varphi}_{1,n_{d,2}}}_{\text{the 2nd domain}} \cdots \underbrace{\boldsymbol{\varphi}_{1,nf-1} \cdots \boldsymbol{\varphi}_{1,n_{d,nf-1}}}_{\text{the } nf-1 \text{ domain}} \underbrace{\boldsymbol{\varphi}_{1,nf} \cdots \boldsymbol{\varphi}_{1,n_{d,nf}}}_{\text{the } nf \text{ domain}} \right] \tag{41}$$

3. Transient quasi-static Ritz vector (TQSRV) method for linear structural analysis

This section is devoted to present a novel set of reduction bases of the TQSRV method for fast transient FE analysis of a complex system. Although the explicit or the implicit solution method employs the *LU* decomposition or similar decomposition methods to avoid repeating factorizations or inversions of effective dynamic stiffness matrices, the transient solution procedure of complex system still takes a lot of computation time even with an advanced engineering software and hardware [4,6–8,33]. Therefore it is our proposition that the MOR scheme can be applied to make the time marching procedure faster.

3.1. The reduction basis for the TQSRV method

Based on our previous contributions and some trials, it is our proposal to combine the reduction bases of the MQSRV method and the reduction bases of the MS method together for a transient FE system as follows:

$$\mathbf{Q} = \left[\underbrace{\boldsymbol{\varphi}_{1,1} \cdots \boldsymbol{\varphi}_{n_{d,1},1}}_{\text{Krylov subspace atthe 1st frequency domain}} \quad \cdots \quad \underbrace{\boldsymbol{\varphi}_{1,nf} \cdots \boldsymbol{\varphi}_{n_{d,nf},nf}}_{\text{Krylov subspace atthenffrequency domain}} \right] \cup [\boldsymbol{\varphi}_{\text{eigen-modes}}] \tag{42}$$

$$n_{d,total} = n_{d,1} + n_{d,2} \cdots n_{d,nf-1} + n_{d,nf} + \text{number of eigenvectors} \tag{43}$$

where the mass orthogonalized bases of the MQSRV method for the ith base at the sth center angular velocity are denoted by $\boldsymbol{\varphi}_{i,s}$. The number of bases at the sth center angular velocity is denoted by $n_{d,s}$. Some eigenvectors orthogonalized with the MQSRV bases are denoted by $\boldsymbol{\varphi}_{\text{eigen-modes}}$. The reason of the above combined bases is that Krylov subspace bases at multifrequencies are effective in a wide range of frequency domains and eigenvector bases are also appropriate in approximating transient motion of structural part. Therefore it is our natural choice to combine these reduction bases for a new MOR method for transient structural system even with the additional computation times for the bases calculation.

Before calculating the bases of the present TQSRV method, at first, the effective way to select center frequencies of the MQSRV method should be considered. The accuracy of an approximated transient solution in frequency domain is improved near to the center frequencies of the present TQSRV method. In other words, the absolute differences between an approximated transient solution of the present TQSRV method and a transient response without the MOR method in frequency domain decrease near at the selected center frequencies. In addition to the selection issue of appropriate center frequencies, the normalization and the orthogonalization of Krylov subspace bases and eigenvectors should be considered. To our best knowledge, in the RV method, the QSRV method, and the MQSRV method, it is an option to apply the so-called mass-orthogonalization process. As eigenvectors are included in the TQSRV method, it is vague whether it is necessary to apply the mass-orthonormalization process or the mathematical orthonormalization process. From some numerical tests, it can be concluded that the mass-orthonormalization is not essential with the eigenvectors and the Krylov subspace bases. This feature will be demonstrated in the numerical section. Finally the following procedure can be developed for the base generation of the TQSRV method.

For the first step, it is assumed that the center angular velocities and the number of bases at each center angular velocities are determined by an engineer or a scientist for a mechanical system of interest. Then at the first center angular velocity domain, the following bases which are same as those of the QSRV method are constructed with the mass orthonormalization process. The first base $\boldsymbol{\varphi}_{1,1}$ at the first center angular velocity, $\omega_{c,1}$, is generated as follows:

$$\boldsymbol{\varphi}_1^* \equiv (\mathbf{K} - \omega_{c,1}^2 \mathbf{M})^{-1} \mathbf{F}, \tag{44}$$

$$\boldsymbol{\varphi}_{1,1} = \frac{1}{\sqrt{\boldsymbol{\varphi}_1^{*\mathrm{T}} \mathrm{M} \boldsymbol{\varphi}_1^*}} \boldsymbol{\varphi}_1^*. \tag{45}$$

Then the next bases are calculated by the following process.

$$\boldsymbol{\varphi}_j^* \equiv (\mathbf{K} - \omega_{c,1}^2\mathbf{M})^{-1}(\mathbf{M}\boldsymbol{\varphi}_{j-1,1}) \quad (j = 2, \cdots, n_{d,1}), \tag{46}$$

$$\boldsymbol{\varphi}_j^{**} \equiv \boldsymbol{\varphi}_j^* - \sum_{k=1}^{j-1}\left(\boldsymbol{\varphi}_{k,1}^{\mathrm{T}}\mathbf{M}\boldsymbol{\varphi}_j^*\right)\boldsymbol{\varphi}_{k,1}, \tag{47}$$

$$\boldsymbol{\varphi}_{j,1} = \frac{1}{\sqrt{\boldsymbol{\varphi}_j^{**\mathrm{T}}\mathbf{M}\boldsymbol{\varphi}_j^{**}}}\boldsymbol{\varphi}_j^{**}. \tag{48}$$

The auxiliary vectors before the mass orthogonalization (47) and before the mass normalization (48) are denoted by $\boldsymbol{\varphi}_j^*$ and $\boldsymbol{\varphi}_j^{**}$, respectively. For the remaining angular velocity domains, the mass orthogonalization and the normalization process with the previous Krylov subspace bases are added to the base generation procedures of the QSRV method. The first base at the sth center angular velocity domain ($s > 1$) is generated as follows:

$$\boldsymbol{\varphi}_1^* \equiv (\mathbf{K} - \omega_{c,s}^2\mathbf{M})^{-1}\mathbf{F} \quad \text{at the } s\text{th center angular velocity}(\omega_{c,s}), \tag{49}$$

$$\boldsymbol{\varphi}_1^{**} \equiv \boldsymbol{\varphi}_1^* - \sum_{p=1}^{s-1}\sum_{k=1}^{n_{d,p}}\left(\boldsymbol{\varphi}_{k,p}^{\mathrm{T}}\mathbf{M}\boldsymbol{\varphi}_1^*\right)\boldsymbol{\varphi}_{k,p} \quad \text{Added orthogonalization procedure}, \tag{50}$$

$$\boldsymbol{\varphi}_{1,s} = \frac{1}{\sqrt{\boldsymbol{\varphi}_1^{**\mathrm{T}}\mathbf{M}\boldsymbol{\varphi}_1^{**}}}\boldsymbol{\varphi}_1^{**}, \tag{51}$$

$$\{s|\text{from 2 to } nf \text{ for the center angular velocity domain index}\}. \tag{52}$$

Note that the procedure (50) is the newly added orthogonalization process that makes the 1st auxiliary Krylov subspace basis at the sth angular velocity domain orthogonal to the previous Krylov subspace bases of the first angular velocity domain to the $(s-1)$th angular velocity domain. After the above steps, the following bases at the sth angular velocity domain are generated

$$\boldsymbol{\varphi}_j^* \equiv \left(\mathbf{K} - \omega_{c,s}^2\mathbf{M}\right)^{-1}(\mathbf{M}\boldsymbol{\varphi}_{j-1,s}) \quad \text{at the } s\text{th center angular velocity } (\omega_{c,s}), \tag{53}$$

$$\boldsymbol{\varphi}_j^{**} \equiv \boldsymbol{\varphi}_j^* - \sum_{p=1}^{s-1}\sum_{k=1}^{n_{d,p}}\left(\boldsymbol{\varphi}_{k,p}^{\mathrm{T}}\mathbf{M}\boldsymbol{\varphi}_j^*\right)\boldsymbol{\varphi}_{k,p} \quad \text{Added orthogonalization procedure}, \tag{54}$$

$$\boldsymbol{\varphi}_j^{***} \equiv \boldsymbol{\varphi}_j^{**} - \sum_{k=1}^{j-1}\left(\boldsymbol{\varphi}_{k,s}^{\mathrm{T}}\mathbf{M}\boldsymbol{\varphi}_j^{**}\right)\boldsymbol{\varphi}_{k,s}, \tag{55}$$

$$\boldsymbol{\varphi}_{j,s} = \frac{1}{\sqrt{\boldsymbol{\varphi}_j^{***\mathrm{T}}\mathbf{M}\boldsymbol{\varphi}_j^{***}}}\boldsymbol{\varphi}_j^{***}, \tag{56}$$

$$\{j|\text{ from 2 to } n_{d,s} \text{ for the } j \text{ th base index at the } s\text{th center angular velocity domain}\}. \tag{57}$$

Table 2
The Newmark scheme with the present TQSRV method.

Calculate the reduction bases ($\boldsymbol{\Phi}$)
Calculate the reduced initial position, the reduced velocity and the reduced acceleration
Calculate the reduced effective stiffness matrix $\left(\mathbf{K}_{\mathrm{Eff}}^{\mathrm{MOR}}\right)$
for time step
$t_{n+1} = t_n + \Delta t$
calculate the current force ($\mathbf{F}_{n+1}^{\mathrm{Eff}}$) and the reduced force ($\mathbf{F}_{\mathrm{Eff}}^{\mathrm{MOR}}$)
calculate the reduced displacements ($\mathbf{Q}_{n+1} \mathbf{K}_{\mathrm{Eff}}^{\mathrm{MOR}} \mathbf{Q}_{n+1} \mathbf{F}_{\mathrm{Eff}}^{\mathrm{MOR}}$)
update the reduced accelerations ($\ddot{\mathbf{Q}}_{n+1}, \ddot{\mathbf{X}}_{n+1} = \boldsymbol{\Phi}\ddot{\mathbf{Q}}_{n+1}$)
update the reduced velocities ($\dot{\mathbf{Q}}_{n+1}, \dot{\mathbf{X}}_{n+1} = \boldsymbol{\Phi}\dot{\mathbf{Q}}_{n+1}$)
end

Once again note that the orthogonalization process of (54) is newly added in order to make the auxiliary base, $\boldsymbol{\varphi}_j^*$, orthogonal to the generated bases at the previous angular velocity domains. And the orthogonalization process and the normalization of the QSRV method of (55) and (56) are performed.

The above generated bases with the mass normalization and the mass orthogonalization processes are good enough to approximate the original response of a finite element model. However, it is found that the inclusion of the bases of the MS method additionally can increase the accuracy of the approximated solution.

Therefore, the following eigenvalue problem is solved for the $n_{d,eig}$ eigenvectors.

$$ {}_{eig}\boldsymbol{\varphi}_j^{\mathrm{T}}\left[\mathbf{K} - {}_{eig}\omega_j^2\mathbf{M}\right]{}_{eig}\boldsymbol{\varphi}_j = 0 \quad (j = 1 \ldots n_{d,eig}, n_{d,eig} \leqslant n_s), \tag{58}$$

where the jth eigenvector and the jth eigen angular velocity are denoted by ${}_{eig}\boldsymbol{\varphi}_j$ and ${}_{eig}\omega_j$, respectively. After that the following orthogonalization process and the normalization process are applied to the eigenvectors before combining to the calculated bases of the MQSRV method.

$$ \boldsymbol{\varphi}_j^{**} \equiv {}_{eig}\boldsymbol{\varphi}_j - \sum_{p=1}^{nf}\sum_{k=1}^{n_{d,p}}(\boldsymbol{\varphi}_{k,p}^{\mathrm{T}}\mathbf{M}_{eig}\boldsymbol{\varphi}_j)\boldsymbol{\varphi}_{k,p} \quad \text{Added orthogonalization procedure}, \tag{59}$$

$$ \boldsymbol{\varphi}_{j,s} = \frac{1}{\sqrt{\boldsymbol{\varphi}_j^{**\mathrm{T}}\mathbf{M}\varphi_j^{**}}}\boldsymbol{\varphi}_j^{**} \quad s = nf + 1, \quad j = 1, \ldots, n_{d,eig} \tag{60}$$

After calculating the above bases of the TQSRV method, the standard reduction process is applied for the Newmark process.

3.2. The Newmark procedure with the TQSRV method

Similar to the application of the other MOR methods, the set of bases of the TQSRV method developed in the Section 3.1 is multiplied before the governing equations but in the time domain (See Table 2). Because the sizes of the active stiffness matrix and the force and the displacement vectors are reduced to $n_{d,total}$ of (61) that is much smaller than the size of the original mechanical system, n_s, the time marching procedure of the Newmark scheme can be accelerated significantly.

$$ n_{d,total} = \sum_{k=1}^{nf} n_{d,k} + n_{d,eig}, \tag{61}$$

$$ \underbrace{\mathbf{K}_{\mathrm{Eff}}^{\mathrm{MOR}}}_{n_{d,total}\times n_{d,total}} = \underbrace{\boldsymbol{\Phi}^{\mathrm{T}}}_{n_{d,total}\times n}\underbrace{K_{\mathrm{Eff}}}_{n\times n}\underbrace{\boldsymbol{\Phi}}_{n\times n_{d,total}}, \underbrace{F_{\mathrm{Eff}}^{\mathrm{MOR}}}_{n_{d,total}\times 1} = \underbrace{\boldsymbol{\Phi}^{\mathrm{T}}}_{n_{d,total}\times n}\underbrace{\mathbf{F}_{n+1}^{\mathrm{Eff}}}_{n\times 1}(n_{d,total} << n_s), \tag{62}$$

$$ \mathbf{K}_{\mathrm{Eff}}^{\mathrm{MOR}}\mathbf{Q}_{n+1} = \mathbf{F}_{\mathrm{Eff}}^{\mathrm{MOR}} \tag{63}$$

$$ \ddot{\mathbf{Q}}_{n+1} = \left(\frac{1}{\beta\Delta t^2}(\mathbf{Q}_{n+1} - \mathbf{Q}_n) - \frac{1}{\beta\Delta t}\dot{\mathbf{Q}}_n + \left(\frac{1}{2} - \beta\right)\ddot{\mathbf{Q}}_n\right), \quad \ddot{\mathbf{X}}_{n+1} = \boldsymbol{\Phi}\ddot{\mathbf{Q}}_{n+1}, \tag{64}$$

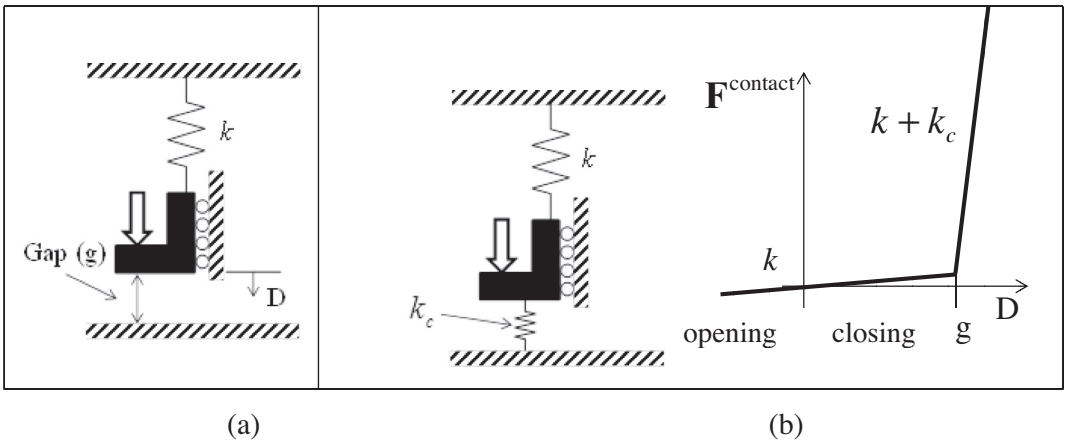

Fig. 3. The stiffness nonlinear spring model for contact. (gap: g, the spring constant: k and the contact spring constant: k_s).

Table 3
The Newmark scheme considering the contact phenomenon.

Set initial position, velocity and acceleration
Calculate the effective stiffness matrix ($\mathbf{K}_{\text{Eff}}$)
for time step
  $t_{n+1} = t_n + \Delta t$
  calculate the current displacements $\left(\mathbf{X}_{n+1}^{\text{Temp}} : \mathbf{K}_{\text{Eff}}\mathbf{X}_{n+1}^{\text{Temp}} = \mathbf{F}_{n+1}^{\text{Eff}}\right)$
  while contact
  calculate the contact force $\left(\mathbf{F}_{n+1}^{\text{Contact}}\right)$
  calculate the current displacements $\left(\mathbf{X}_{n+1}^{\text{Temp}} : \mathbf{K}_{\text{Eff}}\mathbf{X}_{n+1}^{\text{Temp}} = \mathbf{F}_{n+1}^{\text{Eff}} + \mathbf{F}_{n+1}^{\text{Contact}}\right)$
  end
  set the temporary displacements
  to the current displacements $\left(\mathbf{X}_{n+1}^{=}\mathbf{X}_{n+1}^{\text{Temp}}\right)$
  update the accelerations
  update the velocities
end

Table 4
The Newmark scheme considering the contact with the present TQSRV method.

Calculate the reduction bases ($\mathbf{\Phi}$)
Calculate the reduced initial position, the reduced velocity and the reduced acceleration
Calculate the reduced effective stiffness matrix $\left(\mathbf{K}_{\text{Eff}}^{\text{MOR}}\right)$
for time step
  $t_{n+1} = t_n + \Delta t$
  calculate the force $\left(\mathbf{F}_{n+1}^{\text{Eff}}\right)$ and the reduced force $\left(\mathbf{F}_{\text{Eff}}^{\text{MOR}}\right)$
  calculate the reduced auxiliary displacements $\left(\mathbf{Q}_{n+1}^{\text{Temp}} : \mathbf{K}_{\text{Eff}}^{\text{MOR}}\mathbf{X}_{n+1}^{\text{Temp}} = \mathbf{F}_{\text{Eff}}^{\text{MOR}}\right)$
  while contact
  calculate the contact force $\left(\mathbf{F}_{n+1}^{\text{Contact}}\right)$ and the reduced contact force $\left(\mathbf{F}_{n+1}^{\text{Contact,MOR}}\right)$
  calculate the current displacements $\left(\mathbf{Q}_{n+1}^{\text{Temp}} : \mathbf{K}_{\text{Eff}}^{\text{MOR}}\mathbf{X}_{n+1}^{\text{Temp}} = \mathbf{F}_{\text{Eff}}^{\text{MOR}} + \mathbf{F}_{n+1}^{\text{Contact,MOR}}\right)$
  end
  set the auxiliary displacements to the current reduced displacements $\left(\mathbf{Q}_{n+1}^{=}\mathbf{Q}_{n+1}^{\text{Temp}}\right)$
  update the reduced accelerations $\left(\ddot{\mathbf{Q}}_{n+1}\right)$
  update the reduced velocities $\left(\dot{\mathbf{Q}}_{n+1}\right)$
end

$$\dot{\mathbf{Q}}_{n+1} = \dot{\mathbf{Q}}_n + \Delta t(1-\gamma)\ddot{\mathbf{Q}}_n + \gamma\Delta t\ddot{\mathbf{Q}}_{n+1}, \dot{\mathbf{X}}_{n+1} = \mathbf{\Phi}\dot{\mathbf{Q}}_{n+1}, \tag{65}$$

$$\mathbf{X}_{n+1} = \boldsymbol{\varphi}Q_{n+1}, \quad \dot{\mathbf{X}}_{n+1} = \mathbf{\Phi}\dot{\mathbf{Q}}_{n+1}, \ddot{\mathbf{X}}_{n+1} = \mathbf{\Phi}\ddot{\mathbf{Q}}_{n+1}. \tag{66}$$

Not that rather than the backward and the forward substitutions of the *LU* decomposition of the effective stiffness matrix or a direct matrix inversion, the inversion of a small size matrix, $\mathbf{K}_{\text{Eff}}^{\text{MOR}}$, is formulated and the displacement, the velocity and the acceleration updates are also performed in the reduced space in (65). The recoveries of (66) in the real space are performed after the reduced Newmark scheme only if necessary. Therefore although a large finite element model is considered, the above Newmark scheme based on the TQSRV method can make the time marching procedure faster significantly.

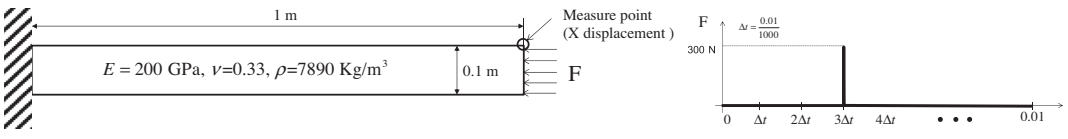

(a) (b)

Fig. 4. A beam structure with a shock wave. (a) An analysis definition (discretized by 120 × 3 QUAD elements) and (b) a force history in time.

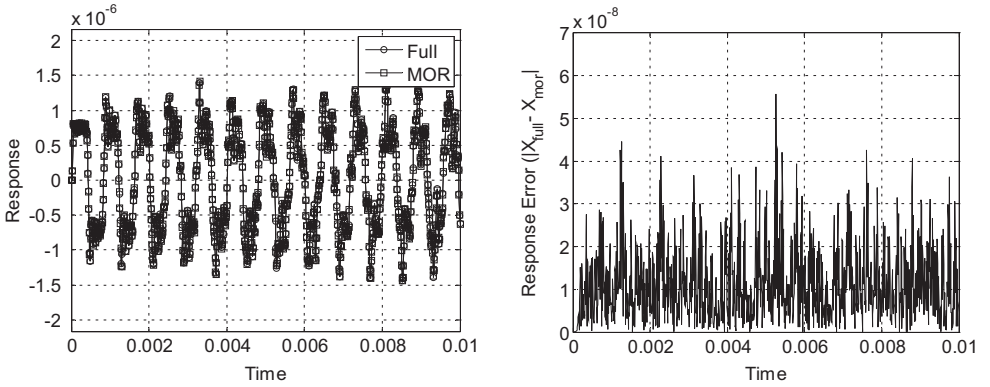

(a) with the mass orthogonalization

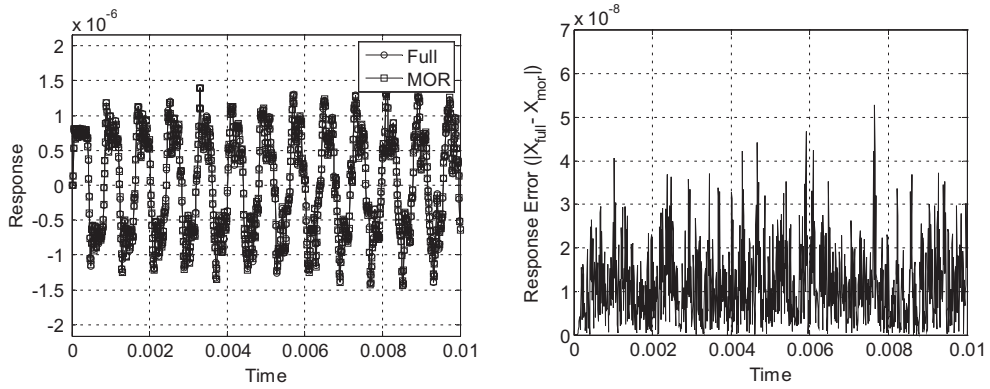

(b) without the mass orthogonalization

Fig. 5. Analysis results with the present TQSRV method without the eigenvectors. (a) The TQSRV method with the mass orthogonalization (Full Newmark analysis: 3.8704 s, TQSRV analysis: 0.6872 s (0.3659 s for bases generation, speedup = 5.6321), center frequencies [0:2000:200000] rad/s, number of bases: 101, 0 eigenvector, $n_{d,s}$=1, (b) (TQSRV analysis: 0.6866 s (0.3587 s for bases generation, speedup = 5.6371) and, center frequencies [0:2000:200000] rad/s, number of bases:101, 0 eigenvector, $n_{d,s}$ = 1).

3.3. The extension for a transient finite element procedure with contact condition

As an extension of the above TQSRV method, it is possible to consider the transient analysis of a mechanical system with contact condition [34]. In the contact analysis, the contact location among structural parts and the magnitude of contact force should be determined that is a very complex task in the FE procedure [1,2]. Because the implementation of all the complex contact algorithms is out of the scope of the paper, the simple nonlinear spring approach of Fig. 3 is implemented as Table 3.

$$\mathbf{K}_{Eff}\mathbf{X}_{n+1} = \mathbf{F}_{n+1}^{Eff} + \mathbf{F}_{n+1}^{Contact} \tag{67}$$

Now the above procedure (Table 3) can be accelerated by the present TQSRV method as Table 4. Unlike the procedure of Table 3, the updates of (67) are performed for every time step in order to check the contact condition in Table 4.

4. Numerical examples

To verify the accuracy and numerical characteristics of the present TQSRV method compared with the existing MOR methods, this section contains several illustrative mechanical examples implemented in the MATLAB environment.

4.1. Example 1: 2D structure with impact

For the first numerical example, a simple beam structure with a shock wave in Fig. 4 is considered. The analysis domain 1 m by 0.1 m is discretized by 120 by 3 QUAD finite elements. Young's modulus, Poisson's ratio and mass density are set to 200 GPa, 0.33 and 7890 kg/m^3, respectively. For a measurement, the x-displacement at the top right node is recorded for the impulse force at 3 Δt .

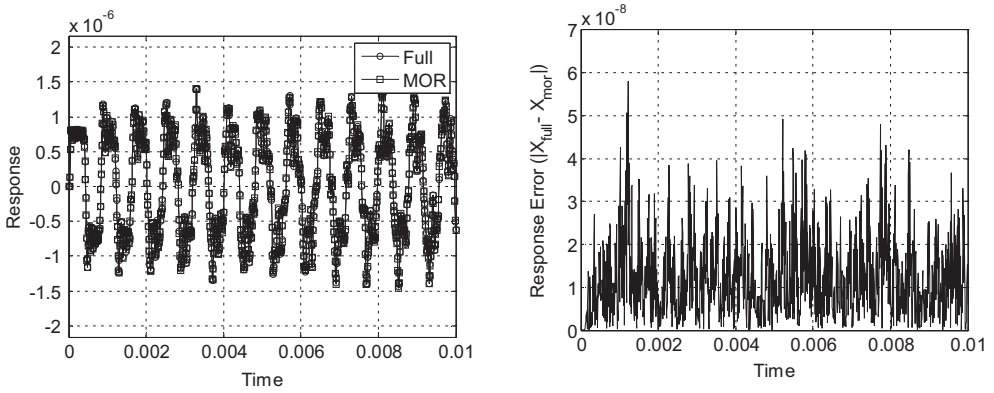

(a) with the mass orthogonalization

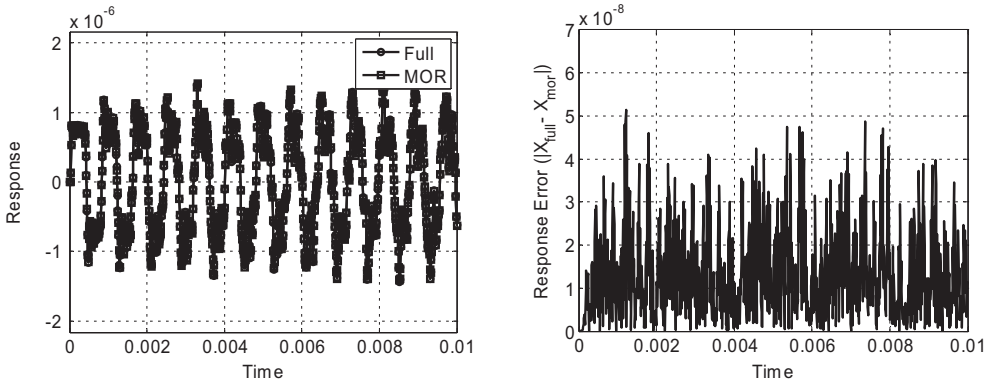

(b) without the mass orthogonalization

Fig. 6. Analysis results with the present TQSRV method with the eigenvectors. (a) The TQSRV method with the mass orthogonalization (Full analysis: 3.8704 s, TQSRV analysis: 0.7739 s (0.3995 s for bases generation) and, center frequencies [0:2000:200000] rad/s, number of bases:101 + 6, 0 eigenvector, $n_{d,s} = 1$), (b) the TQSRV method without the mass orthogonalization (TQSRV analysis: 0.9002 s (0.3800 s for bases generation) and, center frequencies [0:2000:200000] rad/s, number of bases:101 + 6, 0 eigenvector, $n_{d,s} = 1$).

In Fig. 5, the present TQSRV method without the eigenvectors are tested with and without the mass orthogonalization from 0 s to 0.01 s with 10^{-5} s interval. For the TQSRV method, the equal sampled center frequencies from 0 rad/s to 200000 rad/s with 2000 rad/s interval are used and only one basis is generated at each center frequency; the total number of the bases is 101 and they can be regarded as the multifrequency quasi-static Ritz vectors. Mathematically one Krylov subspace basis at a specific center frequency only can accurately represent a constant response but as observed in [3] but the Krylov subspace bases of the other center frequencies also become the acceptable bases for the specific center frequency.

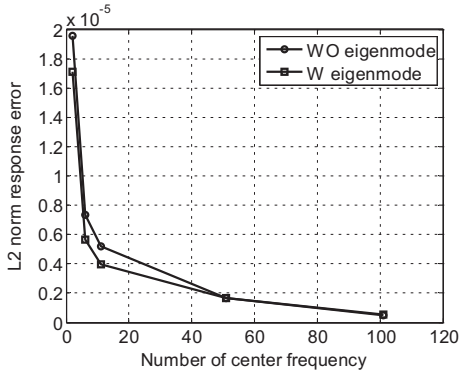

Fig. 7. Test of center frequency domains (Center frequency: [0 2000] rad/s, [0 2000:2000:2000 × 5] rad/s, [0 2000:2000:2000 × 10] rad/s, [0 2000:2000:2000 ×5 0] rad/s, [0 2000:2000:2000 × 100] rad/s).

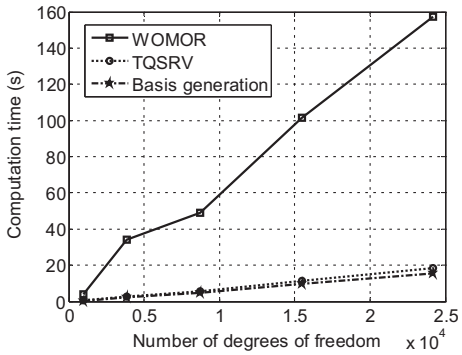

Fig. 8. Speedup test with various meshes without the eigenmode.

Without the TQSRV method referred as the full Newmark analysis, it takes 3.8704 s where the present TQSRV method takes 0.6872 s (0.3659 s for the basis generation and 0.3213 s for the reduced Newmark scheme) with the mass orthogonalization and 0.6866 s without the mass orthogonalization (0.3587 s for the basis generation and 0.3279 s for the Newmark scheme). As illustrated, the almost identical solutions can be obtained over 5 speedup.

On the other hands, the same FE analysis with the additional lowest six eigenvectors is tested in Fig. 6 with and without the mass orthogonalization. It takes a longer time to calculate the eigenvectors compared with the computational time in Fig. 5 but it is observed that it improves the accuracy of the TQSRV method. This also implies that the combined bases of the Krylov subspace bases, the eigenvectors or some other bases if exist require the proper orthogonalization process for the efficient transient FE analysis.

Fig. 7 shows the effect of the number of center frequencies on the accuracy of the present TQSRV method; the L_2 norm errors between the responses of the full Newmark analysis and the TQSRV method are calculated by increasing the center frequencies. As expected, by increasing the number of center frequencies, the higher vibration components of the structural displacements can be represented and naturally the prediction accuracy of the TQSRV method is improved. Furthermore the consideration of the eigenvectors increases the accuracy of the present TQSRV method too especially with the bases at the lower center frequencies.

To test the improvement of the speedup with respect to the size of degrees of freedom, Fig. 8(a) shows the speedup of the present TQSRV method by increasing the number of degrees of freedom. As expected, the more complex the model is, the faster the TQSRV method can solve.

In Fig. 9, the same problem is solved by the MS method. As reported in other relevant researches, the MS method shows the slow convergence because it requires many eigenmodes. In this example, even the 3340 eigenmodes are not sufficient when the rank of the system is 3360. With the 3360 eigenmodes, the original transient responses can be obtained but the time required is 1847 s when 17.4945 s is required with the full analysis.

4.2. Example 2: transient FE analysis for von Mises stress of a beam

For the second numerical example, the transient FE analysis of a beam structure with a constant force (100 lb) in Fig. 10 is considered [2]. The analysis domain 20 in by 1 in is discretized by 40 QUAD FEs. Young's modulus, Poisson's ratio and mass density are set to 30 MPsi, 0.33 and 7.4×10^{-4} lb s^2/in^4, respectively. For a mechanical response, the von Mises stress values at the 21th element are calculated with and without the TQSRV method.

Fig. 11 shows the stress values with the various time step conditions of the TQSRV method. Compared with the analytical solution in [2], the undershoots and the overshoots appear in both the full Newmark scheme and the TQSRV method inevitably. In Fig. 11(a), with $\Delta t = 2.5 \times 10^{-6}$ s for the time incremental step, the full Newmark scheme takes 0.0173 s where the TQSRV method with 51 bases takes 0.1102 s. As the model is too simple, the TQSRV method takes a longer computation time than the full Newmark scheme. In Fig. 11(b), with the same conditions of (a), simply the time increment is decreased to $\Delta t = 2.5 \times 10^{-8}$ s. Thus the full Newmark scheme takes about 68 s where the TQSRV method takes 2 s resulting the speedup over 29. In Fig. 11(c), the number of the TQSRV bases is reduced to 26 and the resulting speedup is over 54. This example shows that the TQSRV method can calculate structural stress values as well as displacements and for a simple FE model, the TQSRV method does not show its computational efficiency as the other MOR methods do.

In Fig. 12, the MS method is applied for the same problem. As shown as the bases of the MS method are the eigenvectors, more than 160 bases should be used. *As reported in other relevant researches, the MS method shows the slow convergence because it requires many eigenmodes.* Furthermore as the reduced effective matrices are full matrices, it takes much more time in this problem.

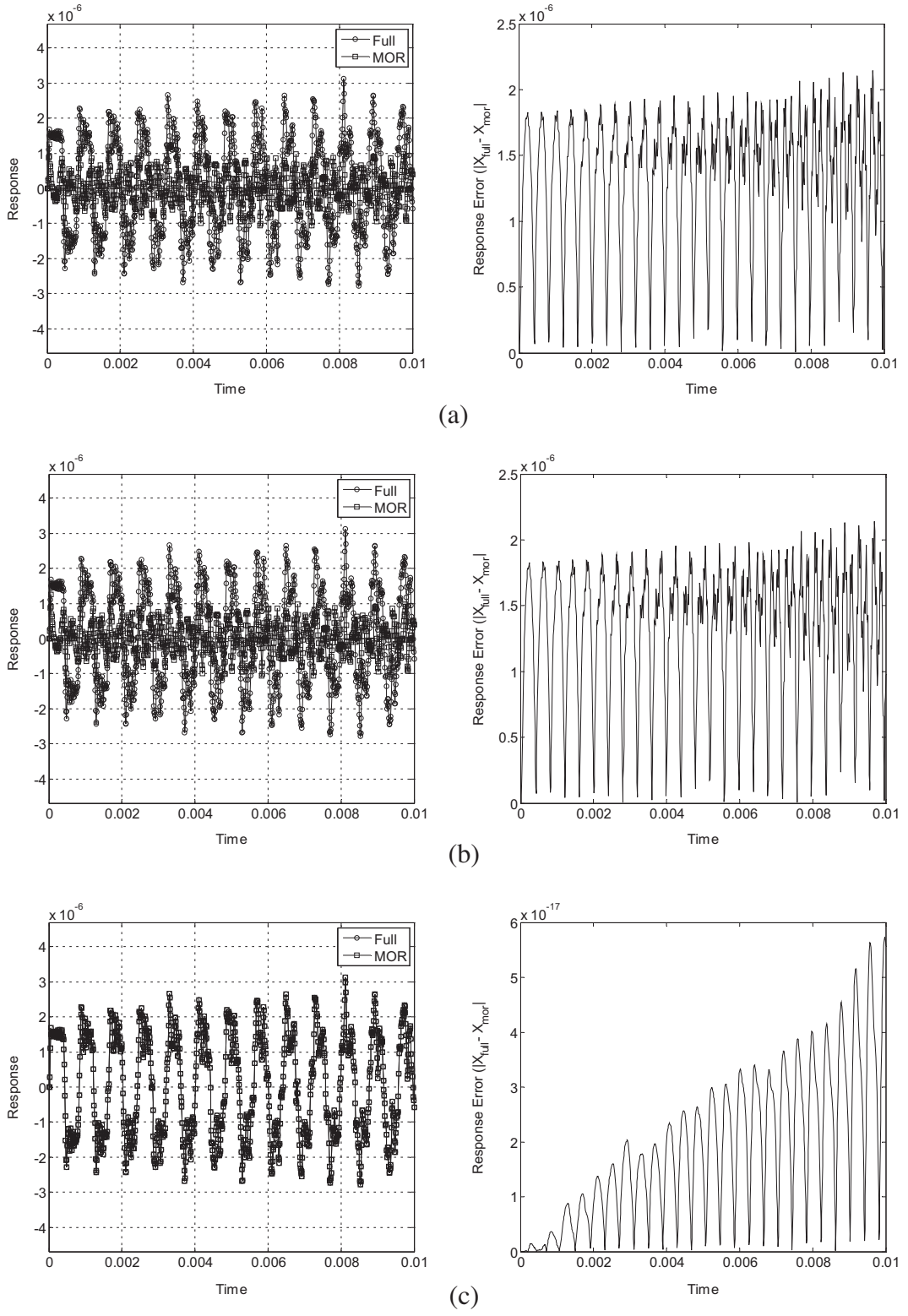

Fig. 9. The stress analysis results with the MS method. (a) the response with the 1000 eigenvalues, $\Delta t = 1.0 \times 10^{-5}$ s, full FE analysis: 17.4945 s, the MS method: 128.4263 s, and (b) the response with the 3340 eigenvalues, $\Delta t = 1.0 \times 10^{-5}$ s, full FE analysis: 17.4945 s, the MS method: 1421.0102 s, (c) the response with the 3360 eigenvalues, $\Delta t = 1.0 \times 10^{-5}$ s, full FE analysis: 17.4945 s, the MS method: 1847.4719 s.

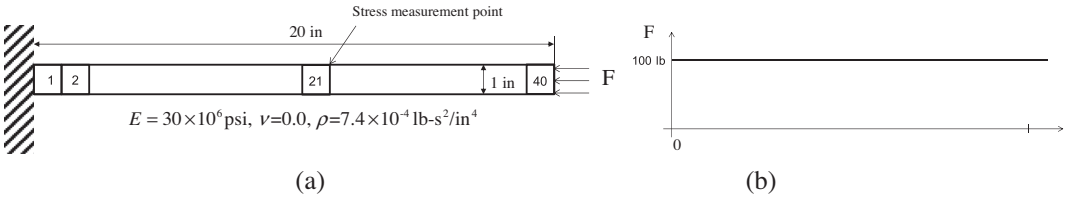

Fig. 10. Transient FE analysis for the von Mises stress for a constant force [2].

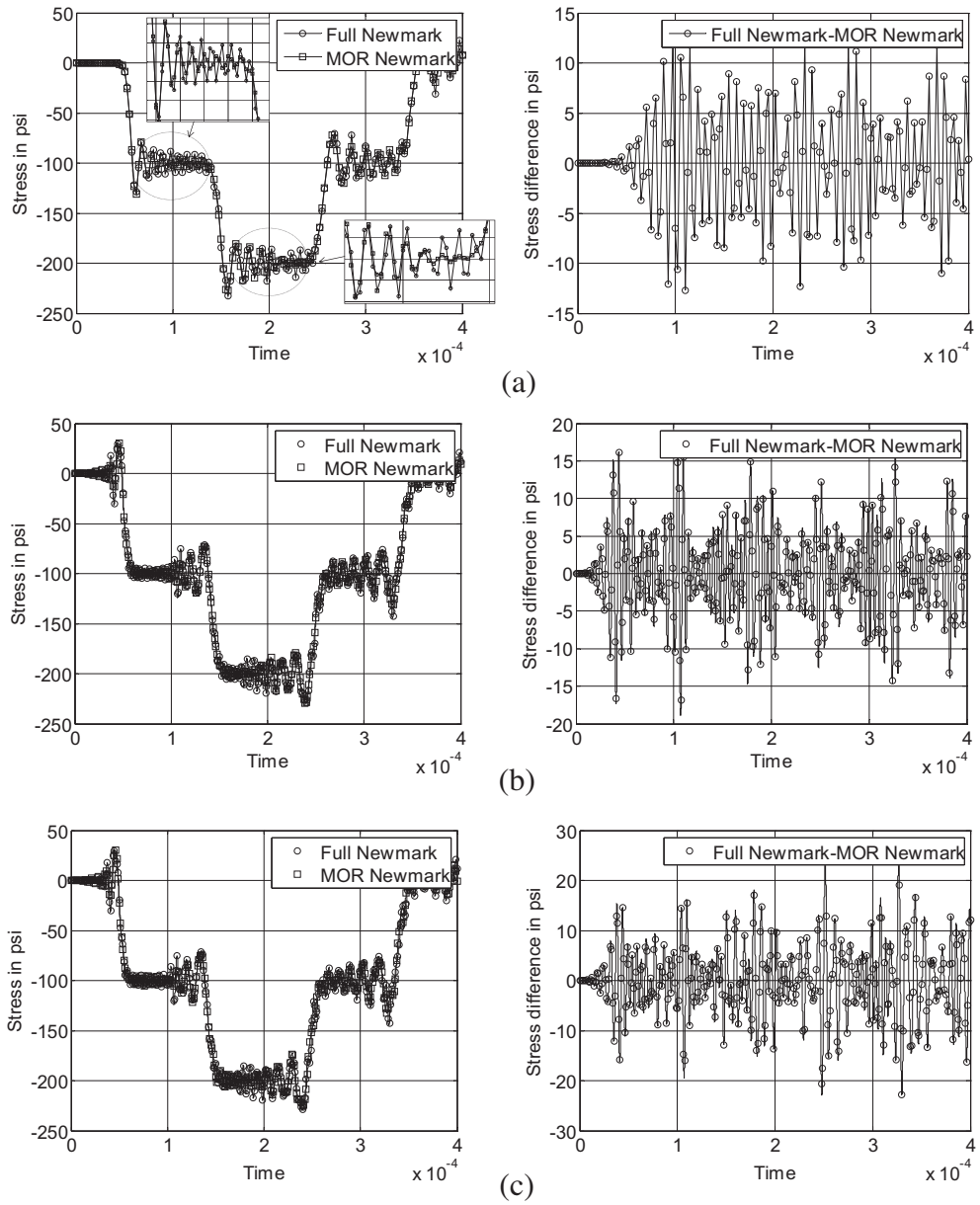

Fig. 11. The stress analysis results with the present TQSRV method. (a) The response with center angular velocity: [0 10000:10000:500000] rad/s, the number of bases: 51, $\Delta t = 2.5\times10^{-6}$ s, full FE analysis: 0.0173 s, the TQSRV method: 0.1102 s, Speedup: 0.1569, (b) the response with center angular velocity: [0 10000:10000:500000] rad/s, the number of bases: 51, $\Delta t = 2.5\times10^{-8}$ s, Full analysis: 68.8576 s, the TQSRV method: 2.3556 s, Speedup: 29.2302, and (c) the response with center angular velocity: [0 20000:20000:500000] rad/s, the number of bases: 26, $\Delta t = 2.5\times10^{-8}$ s, Full analysis: 68.8576 s, the TQSRV method: 1.2632 s, Speedup: 54.5104).

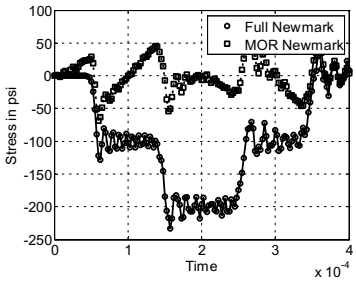

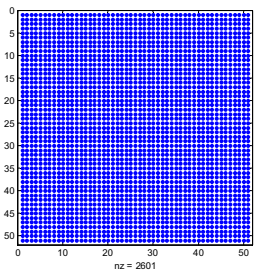

Response ($n_s = 164, n_d = 51$) $\mathbf{K}_{\text{Eff}}^{\text{MOR}}$ (51 by 51)

(a)

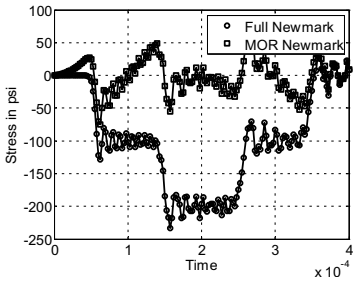

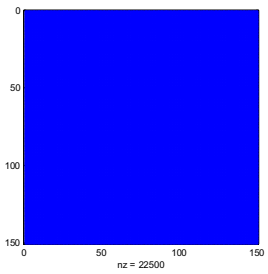

Response ($n_s = 164, n_d = 150$) $\mathbf{K}_{\text{Eff}}^{\text{MOR}}$ (150 by 150)

(b)

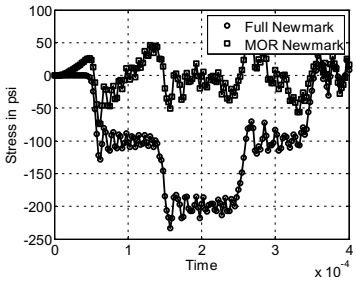

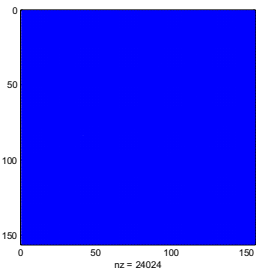

Response ($n_s = 164, n_d = 155$) $\mathbf{K}_{\text{Eff}}^{\text{MOR}}$ (155 by 155)

(c)

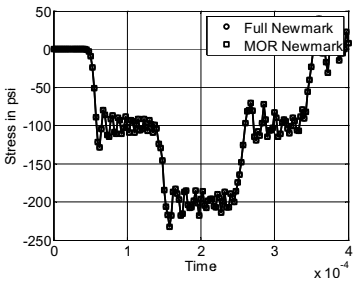

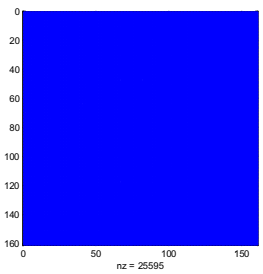

Response ($n_s = 164, n_d = 160$) $\mathbf{K}_{\text{Eff}}^{\text{MOR}}$ (160 by 160)

(d)

Fig. 12. The stress analysis results with the MS method. (a) The response with the 51 eigenvalues, $\Delta t = 2.5 \times 10^{-6}$ s, full FE analysis: 0.0173 s, the MS method: 0.0926 s, (b) the response with the 100 eigenvalues, $\Delta t = 2.5 \times 10^{-6}$ s, full FE analysis: 0.0173 s, the MS method: 0.1687 s, (c) the response with the 150 eigenvalues, $\Delta t = 2.5 \times 10^{-6}$ s, full FE analysis: 0.0173 s, the MS method: 0.3042 s, and (d) the response with the 160 eigenvalues, $\Delta t = 2.5 \times 10^{-6}$ s, full FE analysis: 0.0173 s, the MS method: 0.3252 s.

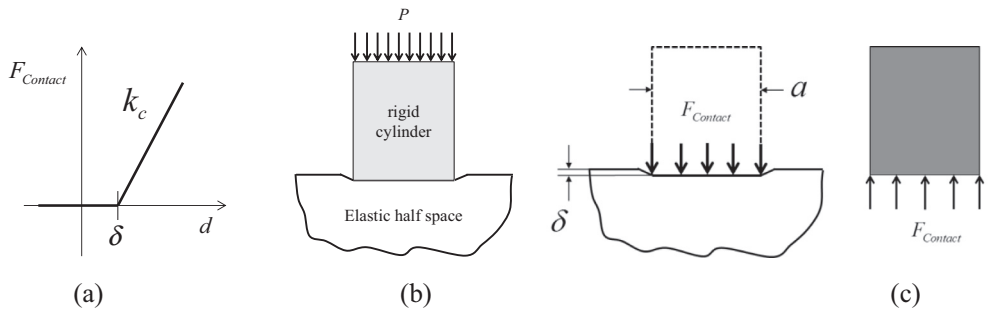

Fig. 13. The contact phenomenon. (the indentation of the elastic foundation:d, $F_{Contact} = \iint_A p(r)drd\theta = 2aE^*\delta$, $p(r) = p_0\left(1-\frac{r^2}{a^2}\right)^{-1/2}$, $\delta = \pi(1-\nu^2)p_0a/E$, $p_0 = \frac{E\delta}{\pi(1-\nu^2)a}$, the Young's moduli of the elastic foundation and the cylinder:$E_1$and E_2, the associated Poisson's ratios: ν_1 and ν_2, the diameter of the cylinder: a, the radius insider the cylinder: r) (a) The contact spring model, (b) the model between a cylinder and an elastic half-space, and (c) the deformation of the elastic foundation and the contact.

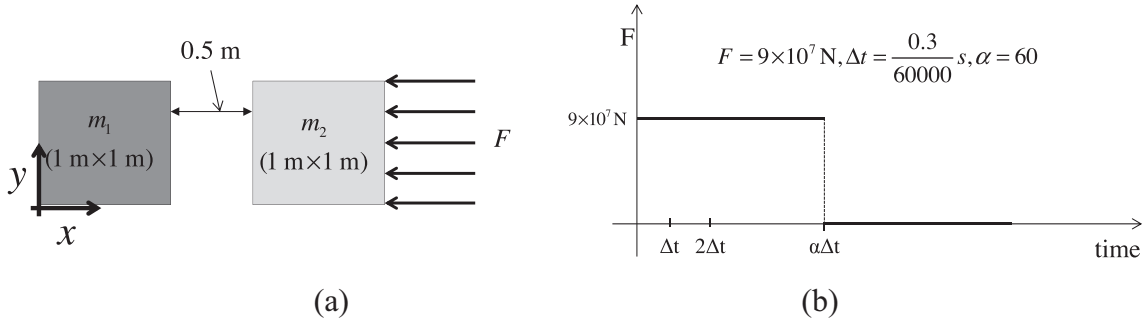

Fig. 14. The contact simulation between two rectangular plane stress boxes. ($m_1, m_2 : E = 200$ GPa, $\nu = 0.3$, $\rho = 7500$ Kg/m^3).

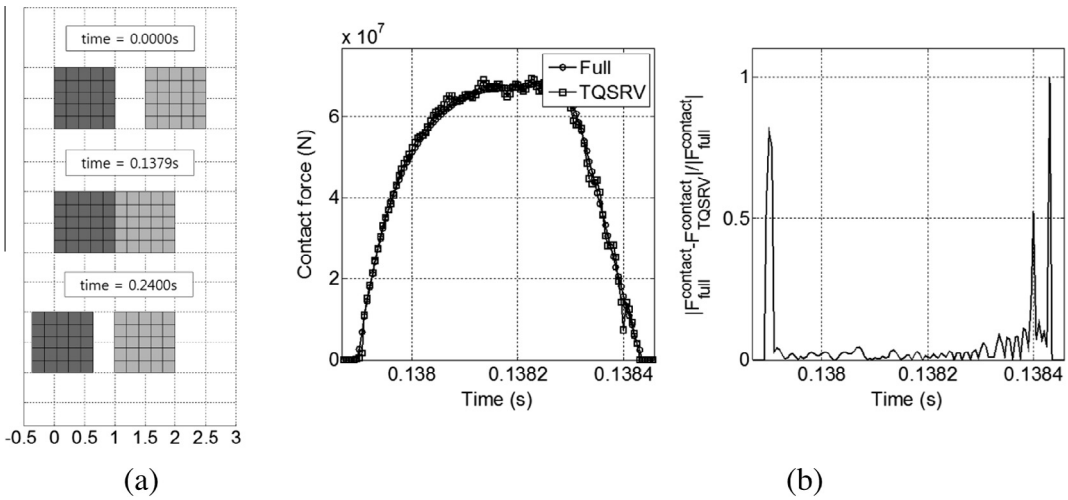

Fig. 15. The collision simulations with the center frequency $[0:1000:10000]$ rad/s. A FE model with DOF: 1764, Time Step: 60000, $CFRE_{full} = 0.1539\%$, $CFRE_{TQSRV} = 0.3795\%$, Full: 23.46 s, TQSRV: 11.34 s, Speedup: 2.050.

4.3. Example 3: Simple contact analysis

4.3.1. The calculation of the simplified contact spring (k_c)

To model the simplified contact model among elastic objects, the contact spring modeling is implemented [2]. In order to derive the contact spring constant, we can consider the contact phenomenon between an elastic cylinder and an elastic half space in Fig. 13.

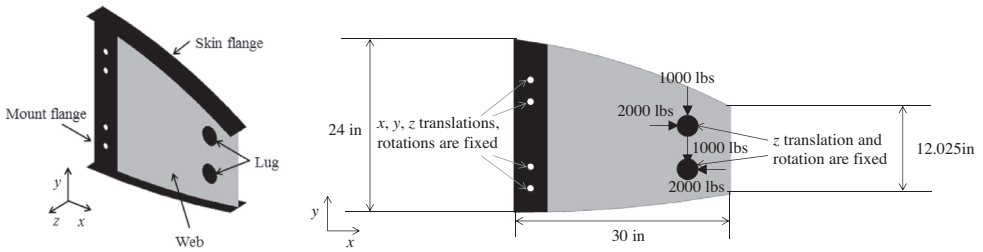

(a)

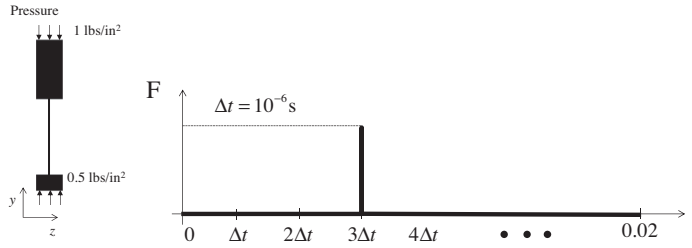

(b)

Time (two X5675 CPU with 12 threads, 24 GB)	Full analysis with multithread solver (parallel)	Full analysis with a single thread *LU* decomposition solver	TQSRV with 500 Krylov bases	TQSRV with 1000 Krylov bases
Basis calculation with 12 threads (s) ([010000:500000] rad/s)			981.2383	1960.3365
Newmark procedure (s)	15777.1674 (4 hours 30 minutes)	180013.9436 (50 hours)	1290.7187	1906.5458
Speedup to multithread[1] and a thread solvers [2]			(6.9475[1],139.4679[2])	(4.0810[1],94.4188[2])

(c)

Fig. 16. A rib model with shell elements.

Then we can derive the simplified contact spring constant as follows:

$$F_{Contact} = k_c\delta, \quad k_c = 2aE^*. \tag{68}$$

What we should emphasize here is that the above is an approximated formulation to estimate the magnitude of the contact spring.

4.3.2. The estimation of simplified initial velocity and momentum

To test the validity of the contact model with the above contact spring, we solve the transient analysis between the two rectangular boxes in the following subsection. The right box is actuated by the external mechanical load in Fig. 14 for 3×10^{-4} seconds and the contact happens between the two boxes. After the contact, the right box moves toward the left side.

To obtain the analytical solutions of the above system, we consider the conservation theories for momentum and energy.

$$m_1V_1 + m_2V_2 = m_1V_1' + m_2V_2', \quad \frac{1}{2}m_1V_1^2 + \frac{1}{2}m_2V_2^2 = \frac{1}{2}m_1V_1'^2 + \frac{1}{2}m_2V_2'^2, \tag{69}$$

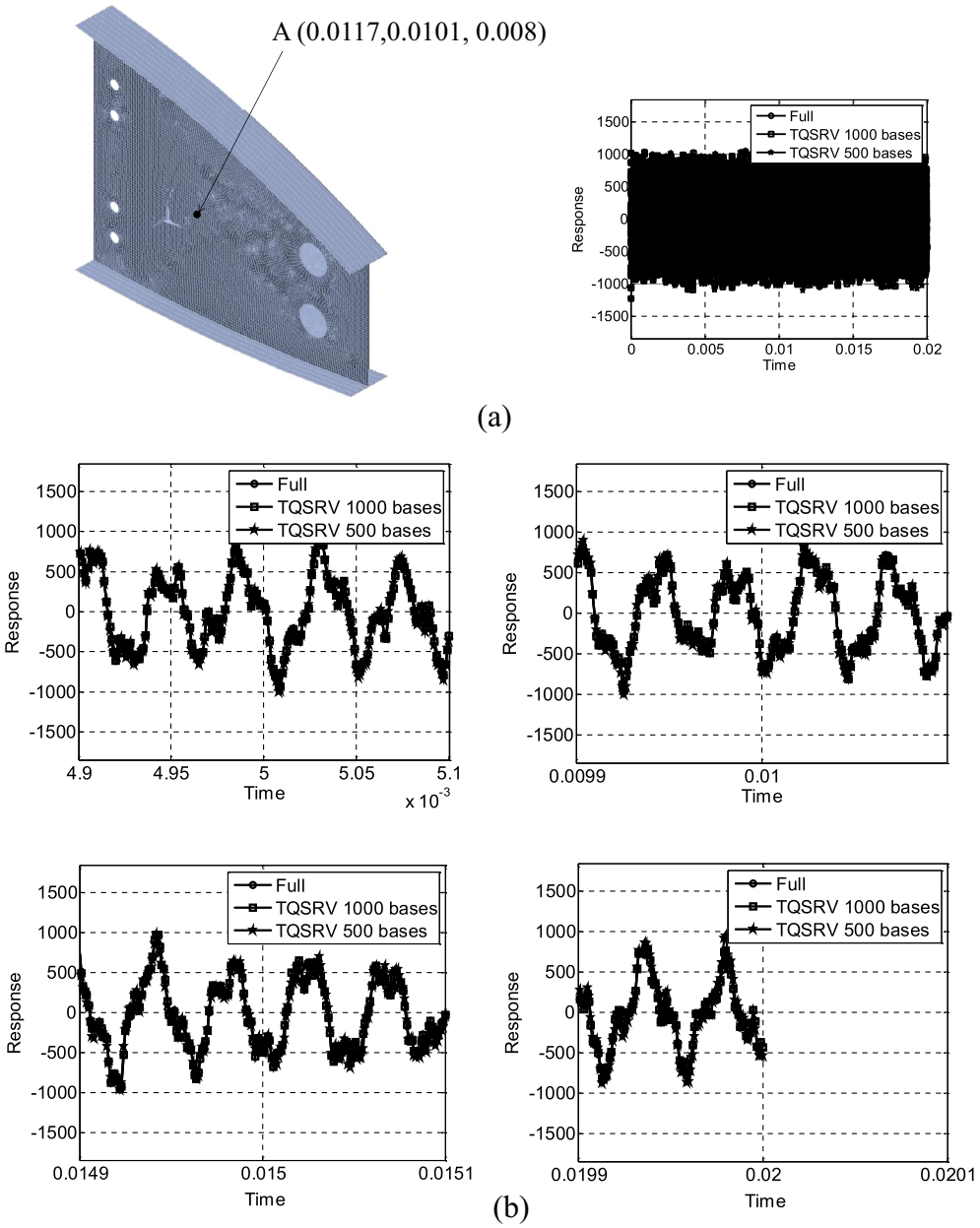

Fig. 17. The analysis results of the rib shell model with the present TQSRV method (the number of DOFs: 90294, 15018 shell elements).

where the velocities before the contact are denoted by V_1 and V_2, and the velocities after the contact phenomenon are denoted by V_1' and V_2', respectively. In case of the equivalent mass values, the velocity solution of the above equation can be obtained as follows:

$$V_1 = 0, V_1' = V_{initial} \quad \text{and} \quad V_2 = V_{initial}, V_2' = 0. \tag{70}$$

The initial velocity just before the contact of the first mass is denoted by $V_{initial}$. To calculate this initial velocity, the applied external force in Fig. 14(b) can be considered in the following Newton's equation.

$$m_2 V_{initial} = -\int_{contact} F_{Contact}\, dt, \quad m_2 V_{initial} = \int F\, dt = \alpha \cdot F \Delta t, \quad \int_{contact} F_{Contact}\, dt = -\alpha F \Delta t, \tag{71}$$

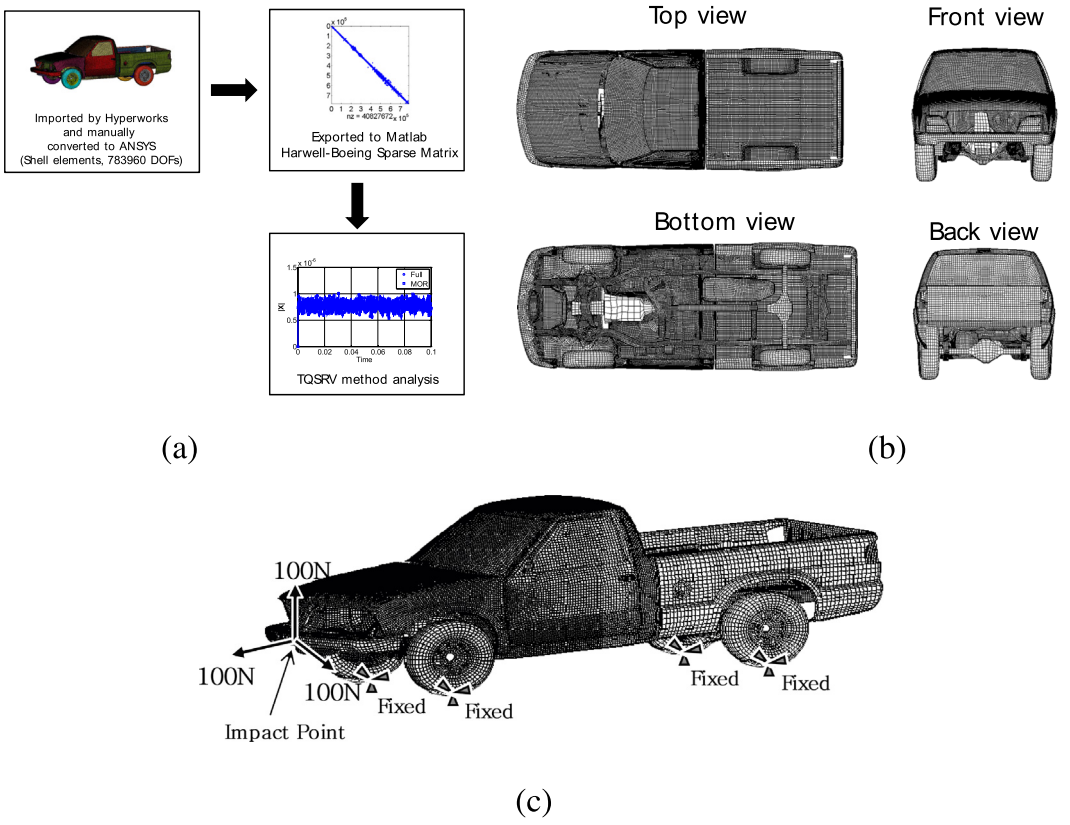

Fig. 18. A transient analysis of an un-tuned automotive FE model (Chevrolet C2500 Pickup). (a) A procedure for the extraction of the stiffness and mass matrices, (b) an employed FE model and (c) the force and boundary conditions.

where the contact force between the two boxes is $F_{Contact}$. The time integration during the contact is defined by $\int_{contact} F_{Contact} dt$. Note by the usage of the integration of the above theoretical contact force, the contact force relative error (CFRE) between the theoretical contact force and the computed contact force can be defined as follows:

$$\mathrm{CFRE} = \frac{\left|\int_{contact} F_{Contact} dt - \int_{contact} F^{FEM}_{Contact} dt\right|}{\left|\int_{contact} F_{Contact} dt\right|} \times 100 = \frac{\left|-\alpha F \Delta t + \sum F^{FEM}_{Contact} \Delta t\right|}{|-\alpha F \Delta t|} \times 100, \tag{72}$$

where the computed contact force in finite element analysis is defined by $F^{FEM}_{Contact}$.

4.3.3. The simulation with the present TQSRV method

The transient collision simulation of the two rectangular boxes is performed by the present TQSRV method in Fig. 15. The magnitudes of the contact force calculated between the two boxes are recorded with the full analysis and the TQSRV method analysis. As illustrated in Fig. 15, the good agreement is obtained between the two analysis methods. The FE model being too simplified, a higher speedup cannot be achievable. Furthermore the computed contact force errors are compared; the area by the envelop of the contact force with respect to time combined with the contact spring constant should be matched with the momentum. The contact force relative errors of the full analysis (CFRE_{full}) and the TQSRV method (CFRE_{TQSRV}) are $\mathrm{CFRE}_{full} = 0.1539\%$ and $\mathrm{CFRE}_{TQSRV} = 0.3795\%$, respectively. Fig. 15(a) shows the displacement histories for some particular times.

4.4. Example 4: Rib FE model

For the next example, the transient FE analysis of the rib of an air plane in Fig. 16 is considered. This rib is modeled with 15018 shell elements and after applying the clamp boundary conditions, the number of the DOFs reduced to 90294. The stiffness matrix and the mass matrix implemented in ANSYS are exported with the functionality of ANSYS to the MATLAB environment. The y direction displacements at (0.0117 m, 0.0101 m, 0.008 m) are calculated and compared for the impact force at $3\Delta t$. Fig. 17 shows the responses at each time and the 1000 bases (1.11% to the total DOFs) and the 500 bases (0.55% to the total DOFs) of the present TQSRV method are good enough to analyze the responses of this complex system with higher speedups.

Time (two X5675 CPU with 12 threads, 24 GB)	Full analysis with multithread solver (parallel)	TQSRV with 115 Krylov bases
Basis calculation with 12 threads (s) (Ritz bases at [0:250:15000] rad/s and 50 eigenmodes)		4305 sec
Newmark procedure (s)	444877 sec (5 days 4 Hours)	6881 sec
Speedup to multithread solver		39.77

(a)

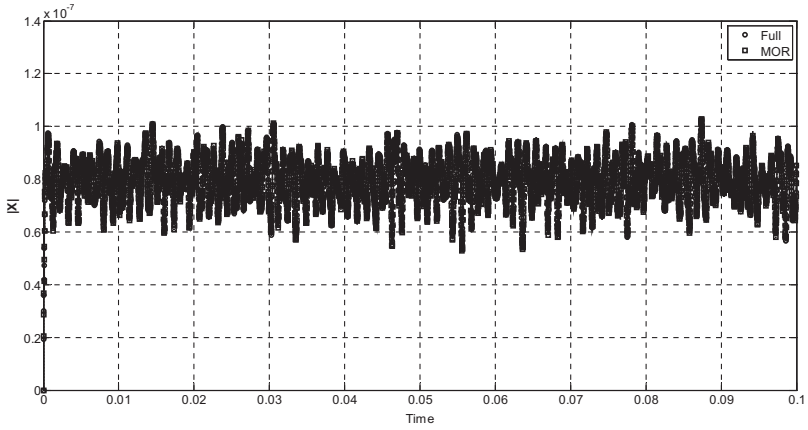

(b)

Fig. 19. The analysis results of the automotive FE model with the present TQSRV method (the number of degrees of freedom: 793,960).

So far, we conduct the numerical examples with the *LU* decomposition method with a single thread solver for the time marching process. In this example, the direct inversions with the 12 threads, a parallel direct solver and the *LU* factorization with a single thread of the effective stiffness matrix of the full Newmark scheme are tested together. As the backward substitution and the forward substitution are performed in a single thread, we found that the parallel direct inversions with the 12 threads can be effective over the *LU* decomposition with a single thread. The details are summarized in Fig. 16(c).

4.5. Example 5: automotive FE model

As a last numerical example, Fig. 18 shows an automotive FE model whose material properties and responses are not verified but just prepared for an illustration purpose (See Fig. 18(a) for the overall procedure). The number of the total degrees of freedom after applying the boundary condition in Fig. 18(c) is 783,960. An impact force is applied to a node at the bumper and the norms of the displacements of the full analysis and the TQSRV method for 0.1 s with 2 μs intervals (50,000 points in time domain) are compared in Fig. 19. For the numerical simulation without the TQSRV method, only the parallel solver is only tried because the single thread solver will takes approximately more than 1230 Hours or 50 days by postulating from the analysis results of the example 4. As shown by applying the present TQSRV method only with 233 bases (approximately 0.0297 % to the original DOFs (783960)), it is possible to solve the system with more than 40 speedup. As stated before, it is crucial to choose proper center frequencies for the Ritz vectors. To choose some center frequencies for this automotive model, we calculate 50 natural frequencies and eigenmodes which are also used in the calculation of the bases of the TQSRV method and we observe that the first natural frequency is about 100 Hz and the 50th natural frequency is about 1195 Hz. Thus we simply calculate the Ritz vector bases from 0 rad/s (static displacement) to 15000 rad/s (approximately 2387 Hz) with 250 rad/s intervals. Only one base is calculated per a center frequency. To show the robustness of the TQSRV method and partially due to the computational time limitation, this crude approach for the center frequencies and the number of bases at each center frequency is tried here. With a refined time step or a wide time span, a much more higher speedup also can be possible. Fig. 19 shows the transient responses and the accurate approximation can be achieved (the norm of the total displacements).

5. Conclusions

The efficient calculation of vibration responses by means of a transient FE procedure is very important in mechanical engineering. By applying a MOR scheme, the active degrees of freedom of complex FE model can be reduced. Although some

existing MOR methods have been developed and applied for frequency response analysis, they are neither very accurate nor effective in transient FE analysis. In order to develop an accurate and effective MOR method for transient FE procedure, this research presents a new MOR method called the transient quasi-static Ritz vector (TQSRV) method whose bases constructed by combining the bases of the MQSRV method and the MS method with and without the mass orthonormalization process.

By solving some benchmark problems and investigating the accuracy and efficiency of the existing RV, QSRV, and MQSRV methods, it can be concluded that the combination of Krylov subspace bases calculated at multiple center frequencies and some eigenvectors of a mechanical system can be very effective for transient FE analysis. It is our conclusion that the transient deformations of a mechanical system due to external dynamic forces with certain frequencies are well described by Krylov subspace bases at the frequencies of external forces. With a shock wave or combined shock, a mechanical system will vibrate in a wide range of frequencies and Krylov subspace bases at wide range frequencies effectively expand its responses. Furthermore, as the vibrating shapes and its dynamic energy spectrum of several lower eigenvectors are dominating from an energy point of view, it was our proposition that the consideration of several lower eigenvectors as well as Krylov subspace bases will be efficient in transient FE analysis. And we observed that the mass orthonormalization process is not essential with the Krylov subspace bases and the eigenvectors of the TQSRV method.

In conclusion, the present TQSRV scheme achieves a significant gain in computational efficiency. With several transient analysis examples, it is found that higher speed-ups can be achieved with the established TQSRV method. One of the remaining issues of the present TQSRV method is establishing robust and systematic approaches for center frequencies and determining the optimal number of Krylov subspace bases associated with center frequencies. We suggest using evenly distributed center frequencies and increasing the number of Krylov subspace bases incrementally while monitoring the accuracy of solutions. For future research topic, the application of the TQSRV method for nonlinear dynamic mechanics should be studied. In the TQSRV method, it is assumed that the dynamic stiffness matrix is not altered during a transient simulation and a fixed time step. By considering the structural nonlinearity and the varying time step condition, this basic assumption is violated and it is vague how to apply the concept of the model order reduction for an efficient transient analysis.

Acknowledgement

This work was supported by the Global Frontier R&D Program on Center for Wave Energy Control based on Metamaterials funded by the National Research Foundation under the Ministry of Science, ICT & Future Planning, Korea (No. 2014063711).

References

[1] K.J. Bathe, Finite Element Procedures, Prentice-Hall, New Jersey, 1996.
[2] R.D. Cook, Concepts and Applications of Finite Element Analysis, 4th ed., Wiley, New York, N.Y., 2002.
[3] G.H. Yoon, Toward a multifrequency quasi-static Ritz vector method for frequency-dependent acoustic system application, Int. J. Numer. Methods Eng. 89 (2012) 1451–1470.
[4] M.S. Yao, Nonlinear structural dynamic finite element analysis using Ritz vector reduced basis method, Shock Vib. 3 (1996) 259–268.
[5] J.M. Ricles, P. Leger, Use of load-dependent vectors for dynamic analysis of large space structures, Commun. Numer. Methods Eng. 9 (1993) 897–908.
[6] P. Leger, S. Dussault, Nonlinear seismic response analysis using vector superposition methods, Earthquake Eng. Struct. D 21 (1992) 163–176.
[7] J.S. Han, E.B. Rudnyi, J.G. Korvink, Efficient optimisation of transient dynamic problems in MEMS devices using model order reduction, J. Micromech. Microeng. 15 (2005) 822–832.
[8] J.M. Gu, Z.D. Ma, G.M. Hulbert, A new load-dependent Ritz vector method for structural dynamics analyses: quasi-static Ritz vectors, Finite Elem. Anal. Des. 36 (2000) 261–278.
[9] I. Kale, J.P. Mackenzie, T.I. Laakso, Motor car acoustic response modelling and order reduction via balanced model truncation, Electron Lett. 32 (1996) 965–966.
[10] G.H. Yoon, Structural topology optimization for frequency response problem using model reduction schemes, Comput. Method Appl. M 199 (2010) 1744–1763.
[11] Z.D. Ma, N. Kikuchi, I. Hagiwara, Structural topology and shape optimization for a frequency-response problem, Comput. Mech. 13 (1993) 157–174.
[12] Z.D. Ma, N. Kikuchi, H.C. Cheng, I. Hagiwara, Topological optimization technique for free-vibration problems, J. Appl. Mech.-Trans. Asme 62 (1995) 200–207.
[13] H. Sohn, K.H. Law, Application of load-dependent Ritz vectors to Bayesian probabilistic damage detection, Probab. Eng. Mech. 15 (2000) 139–153.
[14] B. Anderson, J.E. Bracken, J.B. Manges, G.H. Peng, Z. Cendes, Full-wave analysis in SPICE via model-order reduction, IEEE Trans. Microwave Theory 52 (2004) 2314–2320.
[15] H. Wu, A.C. Cangellaris, Krylov model order reduction of finite element approximations of electromagnetic devices with frequency-dependent material properties, Int. J. Numer. Model. Electron. Networks 20 (2007) 217–235.
[16] T. Breiten, T. Damm, Krylov subspace methods for model order reduction of bilinear control systems, Syst. Control Lett. 59 (2010) 443–450.
[17] T. Watanabe, H. Asai, Macromodel generation for hybrid systems consisting of electromagnetic systems and lumped RLC circuits based on model order reduction, IEICE Trans. Fundam. Electron. E87a (2004) 398–405.
[18] T. Wittig, R. Schuhmann, T. Weiland, Model order reduction for large systems in computational electromagnetics, Linear Algebra Appl. 415 (2006) 499–530.
[19] A.C. Cangellaris, L. Zhao, Model order reduction techniques for electromagnetic macromodelling based on finite methods, Int. J. Numer. Model. Electron. Networks 13 (2000) 181–197.
[20] F.H. Bellamine, A. Elkamel, Model order reduction using neural network principal component analysis and generalized dimensional analysis, Eng. Comput. 25 (2008) 443–463.
[21] M. Alam, A. Nieuwoudt, Y. Massoud, Model order reduction using spline-based dynamic multi-point rational interpolation for passive circuits, Analog Integr. Circuits Signal Process 50 (2007) 273–277.
[22] M.N. Albunni, V. Rischmuller, T. Fritzsche, B. Lohmann, Model-order reduction of moving nonlinear electromagnetic devices, IEEE Trans. Magn. 44 (2008) 1822–1829.
[23] G. Addamo, O.A. Peverini, G. Virone, R. Tascone, R. Orta, Model-order reduction technique for the efficient analysis of complex waveguide structures-an application to the design of corrugated horns, IEEE Antennas Wirel. Propag. 8 (2009) 1039–1042.

[24] E.L. Wilson, A new method of dynamic analysis for linear and nonlinear systems, Finite Elem. Anal. Des. 1 (1985).
[25] M. Ahmadloo, A. Dounavis, Parameterized model-order reduction for efficient eigenanalysis of dielectric waveguide structures, IEEE Trans. Microwave Theory 56 (2008) 2851–2858.
[26] M. Ahmadloo, A. Dounavis, Parameterized model order reduction of electromagnetic systems using multiorder arnoldi, IEEE Trans Adv. Packag. 33 (2010) 1012–1020.
[27] R.W. Aldhaheri, Model order reduction via real schur-form decomposition, Int. J. Control 53 (1991) 709–716.
[28] M.T. Bah, A. Bhaskar, A.J. Keane, Model-order reduction and pass-band based calculations for disordered periodic structures, J. Sound Vib. 256 (2002) 605–627.
[29] I. Balk, S. Zorin, MPI-based parallelized model order reduction algorithm, Lect. Notes Comput. Sci. 3039 (2004) 1012–1016.
[30] S.M. BaniHani, S. De, A comparison of some model order reduction methods for fast simulation of soft tissue response using the point collocation-based method of finite spheres, Eng. Comput. 25 (2009) 37–47.
[31] A.E. Bryson, A. Carrier, 2nd-order algorithm for optimal-model order reduction, J. Guidance Control Dyn. 13 (1990) 887–892.
[32] S.H. Lee, T.Y. Huang, R.B. Wu, Fast waveguide eigenanalysis by wide-band finite-element model-order reduction, IEEE Trans. Microwave Theory 53 (2005) 2552–2558.
[33] O. Ma, J.G. Wang, Model order reduction for impact-contact dynamics simulations of flexible manipulators, Robotica 25 (2007) 397–407.
[34] G.R.J. Guyan, Reduction of stiffness and mass matrices, AIAA J. 3 (1964) 380.
[35] J.S. Han, C. Muller, U. Wallrabe, J.G. Korvink, Design, simulation, and fabrication of a quadstable monolithic mechanism with X- and Y-directional bistable curved beams, J. Mech. Des. 129 (2007) 1198–1203.